Acknowledgment. Work was supported by National Science Foundation (NSF) Grants GP 23267X2 and 38052. Departmental instruments used in this work were supported as follows: NMR, spectrometers, Varian A-60 and HA-100D, E. I. duPont de Nemours and Co., Stauffer Chemical Co., Union Carbide Corp., NSF Grants No. G20207 and GP 8223; Beckman IR-4, E. I. duPont de Nemours and Co., A.E.I. MS9 mass spectrometer, NSF Grant No. GP 3672; Carey 81 Raman spectrophotometer, NSF Grant No. GP-5240. We would like to thank F. A. L. Anet and J. W. Faller for valuable discussions concerning experimentation and interpretation of spin saturation transfer studies discussed in this work.

Supplementary Material Available. A listing of observed and calculated K_{eq} values for $[Ph_4As][Ru_4H_3(CO)_{12}]$ in acetone-d_6 (Table A), THF (Table B), and CH_3OCH_3 (Table C) and temperature profile of rate constants (Table D) will appear following these pages in the microfilm of this volume of the journal. Photocopies of the supplementary material from this paper only or microfiche (105 × 148 mm, 24 × reduction, negatives) containing all of the supplementary material for the papers in this issue may be obtained from the Journals Department, American Chemical Society, 1155 16th St., N.W., Washington, D.C. 20036. Remit check or money order for $4.00 for photocopy or $2.50 for microfiche, referring to code number JACS 75-3947.

References and Notes

(1) (a) Work presented at the 165th National Meeting of the American Chemical Society, Dallas, Texas, April 8–13, 1973, Abstracts, paper INOR 33; (b) taken in part from the Dissertation of J. W. Koepke, UCLA, Dec 1974.
(2) S. A. R. Knox and H. D. Kaesz, *J. Am. Chem. Soc.*, **93**, 4594 (1971).
(3) H. D. Kaesz, *Chem. Brit.*, **9**, 344 (1973).
(4) See paragraph at the end of this article regarding supplementary material or ref 1b.
(5) R. L. Lipnick and E. W. Garbisch, Jr., *J. Am. Chem. Soc.*, **95**, 6375 (1973).
(6) G. J. Karabatsos, D. J. Fenoglio, and S. S. Lande, *J. Am. Chem. Soc.*, **91**, 3572 (1969).
(7) B. L. Edgar, D. J. Duffy, M. C. Palazzotto, and L. H. Pignolet, *J. Am. Chem. Soc.*, **95**, 1125 (1973).
(8) (a) See discussion in Y. Lim and R. S. Drago, *J. Am. Chem. Soc.*, **94**, 84 (1972), and references cited therein; (b) J. Smid, *Angew Chem., Int. Ed. Engl.*, **11**, 112 (1972).
(9) W. F. Edgell and N. Pauuwe, *Chem. Commun.*, 284 (1969).
(10) E. E. Eliel and O. Hofer, *J. Am. Chem. Soc.*, **95**, 8041 (1973).
(11) P. Meakin, E. L. Muetterties, and J. P. Jesson, *J. Am. Chem. Soc.*, **95**, 75 (1973).
(12) J. W. Faller in "Determination of Organic Structures by Physical Methods", Vol. 5, F. C. Nachod and J. J. Zuckerman, Ed., Academic Press, New York, N.Y., 1973, pp 75–97.
(13) (a) H. D. Kaesz, S. A. R. Knox, J. W. Koepke, and R. B. Saillant, *Chem. Commun.*, 477 (1971); (b) see S. A. R. Knox, J. W. Koepke, M. A. Andrews, and H. D. Kaesz, *J. Am. Chem. Soc.*, preceding paper in this issue.
(14) Heather King, UCLA.
(15) (a) M. Saunders and E. L. Hagen, *J. Am. Chem. Soc.*, **90**, 6881 (1968); (b) adapted for use on IBM 360 machines by P. M. Henrichs, Ph.D. Thesis, U.C.L.A., 1969, with extension to include iterative fitting by William Larson of UCLA Chemistry Department.

Unusual Metalloporphyrin Complexes of Rhenium and Technetium[1]

M. Tsutsui,*[2a] C. P. Hrung,[2a] D. Ostfeld,[2a] T. S. Srivastava,[2a] D. L. Cullen,[2b] and E. F. Meyer, Jr.[2b]

Contribution from the Department of Chemistry, and the Department of Biochemistry and Biophysics, Texas Agricultural Experiment Station, Texas A&M University, College Station, Texas 77843. *Received December 4, 1974*

Abstract: By reaction of dirhenium decacarbonyl, $Re_2(CO)_{10}$, or ditechnetium decacarbonyl, $Tc_2(CO)_{10}$, with mesoporphyrin IX dimethyl ester, H_2MPIXDME, or *meso*-tetraphenylporphine, H_2TPP, monometallic and bimetallic porphyrin complexes of rhenium and technetium were synthesized. Visible spectroscopy indicates that first the monometallic and then the bimetallic porphyrin complex is formed. The monometallic complex of rhenium can further react with either $Re_2(CO)_{10}$ or $Tc_2(CO)_{10}$ to form the homo- and heterodinuclear metalloporphyrin complexes. Structural data for the homodinuclear metalloporphyrin complexes of both rhenium and technetium, TPP$[Re(CO)_3]_2$ and TPP$[Tc(CO)_3]_2$, were obtained by single-crystal X-ray diffraction. Both the rhenium and technetium homodinuclear porphyrins are centrosymmetric complexes having two metals bonded to the porphyrin, one above and one below the plane of the macrocycle while the porphyrin macrocycle is highly distorted. The metal ions are not positioned directly over the center of the macrocycle but are set to one side such that each metal ion is bonded to three nitrogen atoms. There is a small but significant difference in the metal–metal distance, with the Tc–Tc distance being 0.02 Å shorter. The M–M distance (3.101 Å for the Tc complex) though somewhat long for bonding is short enough that some metal–metal interaction may be possible. Due to the observed similarity in both their chemical and physical properties, it was assumed that not only the homo- and heterodinuclear metalloporphyrins but also the monometallic porphyrin complexes of Re and Tc have similar structures. Proton magnetic resonance spectrum of (H-TPP)$Re(CO)_3$ gave evidence for the proposed structure of the monometallic porphyrin complexes. In the monometallic complexes, the porphyrin acts as a tridentate instead of a tetradentate ligand, while in the bimetallic complexes the porphyrin acts as a hexadentate ligand; both of these are considered nonclassical coordination numbers for the porphyrin ligand. A fluxional character of both Re and Tc monometallic porphyrin complexes was observed by variable-temperature ^{1}H NMR spectral studies. This fluxional phenomenon is best explained by the intramolecular rearrangement of the metal–carbonyl group among the four ring nitrogen atoms of porphyrin and a concomitant movement of the N–H proton. A novel thermal disproportionation of (H-MP)$Tc(CO)_3$ to MP$[Tc(CO)_3]_2$ and H_2MPIXDME was also observed. A dissociation and recombination of the metal–carbonyl moieties and the porphyrin ligands between two of the (H-MP)$Tc(CO)_3$ molecules would seem interpretable for this unusual coordination phenomenon.

There is a growing interest in metalloporphyrins because of the unique nature of the coordination chemistry of these materials[3-8] and also because of their obvious relevance as biological models[9-12] (such as chlorophyll,[13] hemoglobin,[14] cytochrome,[15] and vitamin B_{12}[16,17]). Changes or modification of general porphyrin metabolism are associated with

cancer, drug metabolism, and specific disease syndromes.[18] Thus, the biological functions of metalloporphyrins are of a great deal of importance. Most of the research in metalloporphyrins not only stems from interest in the biological systems to which they are related but also stems from the search for new semiconductors,[19] superconductors,[20] anticancer drugs,[21] tumor localization agents,[22] and catalysts.[23] Even without their biological and industrial implications the properties and a large variety of structural types[4] of metalloporphyrins would be studied for their purely theoretical importance.

Understanding of the porphyrin system has advanced appreciably in recent years.[8] Except for lanthanides[24] and actinides, almost every metal in the periodic table has been coordinated to a porphyrin.[7] Any reasonable porphyrin complex desired by inorganic chemists seems attainable through the powerful synthetic methods which are now available. These methods included: (1) reaction of a porphyrin with a metallic salt (acetate, halide, oxide, etc.) in an acidic or basic medium;[3] (2) supplying the metal in the form of carbonyls,[25,26] carbonyl halides,[27,28] or other organometallic compounds;[26,29] (3) the use of an acetylacetonate complex[24,30] as a source of metal; (4) reaction in a medium of high dielectric constant (such as phenol, benzonitrile, *N,N*-dimethylformamide, etc.).[31,32]

The major problem in the traditional metalloporphyrin syntheses is that of the difficulty in dissolving both the free porphyrin and the metallic salt simultaneously into the same solution under reactive conditions.[3] This is due to the fact that good solvents for the porphyrins in their un-ionized forms are generally poor solvents for simple metallic ions and vice versa. In an acidic medium, the porphyrin exists mostly in the unreactive protonated form. In a basic medium, on the other hand, the porphyrin must compete (often disadvantageously) with the solvent as a complexing agent for the metal ion. The solubility problem was overcome by using high dielectric solvents which are capable of dissolving both the free porphyrin and the metallic salt. It is general, rapid, and convenient, gives high and large yields, and requires no special reagents. This method was developed by Adler[31] and further extended by Buchler[32] for the preparation of a number of previously unknown metalloporphyrin complexes of scandium,[30] zirconium,[30] hafnium,[32] niobium,[32] tantalum,[32] tungsten,[33] rhenium,[33] and osmium.[34] These new metalloporphyrins have been used to demonstrate the geometric limits of the porphyrin ligand[32] as well as some additional geometries which it can assume.[35] It is of interest that metal acetylacetonates are found both readily available and reasonably soluble in nonpolar organic solvents, and are therefore used as a useful metal source for the preparation of new metalloporphyrins.[24,30,35] The solubility problem in the synthesis of metalloporphyrins was also overcome by the use of organometallic compounds as the metal source,[26,29] but the inconvenience involved in obtaining air-sensitive organometallic derivatives and the availability of other methods have prevented greater use of the organometallics as starting materials.

The use of metal carbonyls for the insertion of metal ions into porphyrins was introduced by Tsutsui[25] in 1966. This method has been found quite general for metals having suitable derivatives and developed to an useful and unique method in the syntheses of unusual metalloporphyrins within the last decade.[7] In addition to a number of previously reported metalloporphyrins, the reaction of metal carbonyls or metal carbonyl halides with neutral porphyrins has led to the syntheses of new metalloporphyrin complexes of chromium,[25,36] molybdenum,[36,37] ruthenium,[28,38] rhodium,[39-42] iridium,[27,29] rhenium,[43,44] and technetium.[45,46] Except for the chromium and molybdenum porphyrin complexes, carbonyl groups are retained by the metals in the new metalloporphyrins. For rhodium, rhenium, and technetium metalloporphyrins, unusual bimetallic complexes with a low oxidation state and out-of-plane structure were obtained for the first time. The unusual bimetallic rhodium complex and its derivatives were reported by Yoshida and coworkers.[40-42] More detailed spectral and structural data for the unusual monometallic and bimetallic rhenium and technetium porphyrin complexes are described and compared in this paper. Both the out-of-plane rhenium and technetium bimetallic complexes of *meso*-tetraphenylporphine are isostructural. The single-crystal X-ray diffraction analysis data obtained for the technetium complex is superior to that obtained for the rhenium complex. Absorption effects are much smaller in the former, and the metal ion contributes to a smaller percentage of the scattering power, which means the nonmetal atoms can be located with much more accuracy. As a result more may be said about the structural details of the porphyrin macrocycle.

Results

Unusual Rhenium Metalloporphyrin Complexes. Reflux of decalin solutions containing $Re_2(CO)_{10}$ and porphyrin has given several different rhenium porphyrins, depending on the ratios of reactants and on the porphyrin used. Among the compounds isolated were: (monohydrogen mesoporphyrin IX dimethyl esterato)tricarbonylrhenium(I), $HMPRe(CO)_3$ (I); (monohydrogen *meso*-tetraphenylporphinato)tricarbonylrhenium(I), $HTPPRe(CO)_3$ (II); μ-[mesoporphyrin IX dimethyl esterato]-bis[tricarbonylrhenium(I)], $MP[Re(CO)_3]_2$ (III); μ-[*meso*-tetraphenylporphinato]-bis[tricarbonylrhenium(I)], $TPP[Re(CO)_3]_2$ (IV).

The characterization of these compounds was done by elemental analyses, visible, infrared, proton magnetic resonance, and mass spectra (Tables I and II).

Compound II was particularly appropriate for ^1H NMR studies. Its ^1H NMR spectrum in deuteriochloroform showed an upfield singlet at δ −4.0 for the N-H proton, two broad multiplets at 7.87 and 8.30 for the phenyl protons, and three sets of signals (Figure 1) for the β-pyrrole protons. The peaks due to the β protons include an AB quartet[47] centered at 9.11 (J_{AB} = 5.0 Hz, with a ratio between the outer and the inner peaks of 1:2.2), a doublet centered at 8.88 (J = 2.0 Hz), and a singlet centered at 8.72. The relative intensities of these sets of peaks were 2:1:1. This is consistent with coordination between the rhenium atom and the nitrogen atoms of three adjacent pyrroles (rings B, C, and D of Figure 2). The uncoordinated pyrrole nitrogen atom (ring A in Figure 2) would be bound to a proton. This proton would cause the splitting observed at 8.88 and was completely exchangeable with deuterium. In the deuterated sample the doublet centered at 8.88 collapsed to a singlet of about twice the peak height but the same area. This type of coordination was found for each metal ion in the X-ray determination of the structure of the bimetallic complex IV.[44]

Compound III was also prepared by the reaction of $H_2MPIXDME$ with excess $Re_2(CO)_{10}$ in refluxing decalin under argon. The reaction occurred in a stepwise manner by forming complex I as reaction intermediate. This phenomenon was detected by a stepwise change of visible absorption spectra (Figure 3) and a continuous change of color in the reaction mixture (from an initial reddish purple color to greenish brown and finally to a dark reddish brown color). However, this stepwise reaction is not reversible. Attempts at the conversion of III to I by reflux in decalin with excess $H_2MPIXDME$ were unsuccessful. The formation of these two unusual rhenium metalloporphyrin complexes is seen to

Table I. Spectral Data for Unusual Metalloporphyrin Complexes, I–IX

No.	Compound	Mp (°C)	Uv, ν_{max}, nm (log ϵ) (in CH_2Cl_2)	Ir, cm^{-1} (KBr pellet)	^1H NMR (δ) (in $CDCl_3$)
I	(H-MP)Re(CO)$_3$	175–177	388 (Soret) 480 580	1740 (ester, CO) 1880 (ν(M–CO)) 2020 (ν(M–CO)) 3380 (ν(N–H))	10.5 (s), ═CH– 10.2 (s), ═CH– 4.7–3.0 (m), alkyl 2.0–1.6 (t), alkyl –4.9 (s), NH
II	(H-TPP)Re(CO)$_3$	302–304	402 (6.12) 473 (5.62) 670 (4.92)	1875 (ν(M–CO)) 2010 (ν(M–CO)) 3350 (ν(N–H))	9.13 (q), pyrrole 8.88 (d), pyrrole 8.72 (s), pyrrole 8.30 (m), phenyl 7.87 (m), phenyl –4.00 (s), NH
III	MP[Re(CO)$_3$]$_2$	246–248	400 (Soret) 480 sh 520	1730 (ester, CO) 1900 (ν(M–CO)) 2015 (ν(M–CO))	10.30 (s), ═CH– 4.7–3.0 (m), alkyl 2.0–1.6 (t), alkyl
IV	TPP[Re(CO)$_3$]$_2$	350 dec	408 (Soret) 485 sh 513	1900 (ν(M–CO)) 2025 (ν(M–CO))	9.20 (s), pyrrole 8.30 (m), phenyl 7.80 (m), phenyl
V	(OC)$_3$ReMPTc(CO)$_3$	238–240	398 (5.04) 480 sh (3.80) 513 (4.46)	1720 (ester, CO) 1740 (ester, CO) 1925 (ν(M–CO)) 2030 (ν(M–CO)) 2045 (ν(M–CO))	10.60 (s), ═CH– 4.7–3.0 (m), alkyl 2.0–1.5 (m), alkyl
VI	(H-MP)Tc(CO)$_3$	181–182	388 (4.17) 473 (3.70) 580 (3.17)	1735 (ester, CO) 1900 (ν(M–CO)) 1920 (ν(M–CO)) 2025 (ν(M–CO)) 3380 (ν(N–H)	10.5 (s), ═CH– 10.2 (s), ═CH– 4.7–3.0 (m), alkyl 2.0–1.6 (t), alkyl –4.90 (s), NH
VII	MP[Tc(CO)$_3$]$_2$	227–229	396 (4.43) 480 (3.60) 507 (3.93)	1740 (ester, CO) 1925 (ν(M–CO)) 2036 (ν(M–CO))	10.40 (s), ═CH– 4.7–3.0 (m), alkyl 2.0–1.7 (t), alkyl
VIII	TPP[Tc(CO)$_3$]$_2$	323–325	403 nm (Soret) 475 sh 504 670	1915 (ν(M–CO)) 2030 (ν(M–CO))	
IX	Unknown derivative of VII	260, dec	358 nm 397 (Soret) 500 540	1725 (ester, CO) 1925 (ν(M–CO)) 2044 (ν(M–CO))	

Table II. Relative Intensities of Ion Species of Interest in the Mass Spectra of Complexes I and III

Ion Species	Relative intensities (H-MP)Re(CO)$_3$	Relative intensities MP[Re(CO)$_3$]$_2$
$(M)^+$	8.8	43.80
$(M - H)^+$	0.54	0.60
$(M - 2H)^+$	0.08	0.20
$(M - CH_3O)^+$	1.80	4.00
$(M - 2CO)^+$	0.25	5.30
$(M - CH_3CO_2)^+$	0.43	1.30
$(M - 3CO)^+$	100.00	
$(M - 3CO - H)^+$	1.20	
$(M - 5CO)^+$		100.00
$(M - 5CO - H)^+$		1.40
$(M - 6CO)^+$		68.90
$(M - 6CO - H)^+$		1.50
$(M)^{2+}$		2.50
$(M - 3CO)^{2+}$	27.20	
$(M - 4CO)^{2+}$		47.60
Isotope peaks of parent ion		
M	1.00	1.00
M + 1	0.50	0.59
M + 2	1.79	3.60
M + 3	0.77	1.71
M + 4		3.26
M + 5		1.38

proceed via the following reaction scheme, where MP represents the dianion of mesoporphyrin IX dimethyl ester.

$$H_2MP + Re_2(CO)_{10} \xrightarrow{\Delta} MP[Re(CO)_3]_2 + H_2\uparrow + 4CO\uparrow \quad (1)$$

$$2H_2MP + Re_2(CO)_{10} \xrightarrow{\Delta} 2(H\text{-}MP)Re(CO)_3 + H_2\uparrow + 4CO\uparrow \quad (2)$$

$$2(H\text{-}MP)Re(CO)_3 + Re_2(CO)_{10} \xrightarrow{\Delta} 2MP[Re(CO)_3]_2 + H_2\uparrow + 4CO\uparrow \quad (3)$$

Derivatives of Monorhenium Metalloporphyrin Complex. The reaction of I with excess $Re_2(CO)_{10}$ to form the dirhenium complex, III, suggested the possibility of making a series of complexes in which the porphyrin ring is bound to both rhenium atom and an atom of another metal. Although this could not be done with all metals, I did react further with several mono- and divalent cations of heavy metals (Ag^+, Hg^{2+}, and Pb^{2+}) in a basic solvent.[48] Evidence for these reactions came from changes in the visible absorption spectra of the solutions (Table III). It is presumed that monovalent cations replace the remaining pyrrole proton of I, forming a 1:1 complex. Divalent cations are thought similarly to replace a pyrrole proton from each of two molecules of I, forming a sandwich-type complex with the heavy metal ion situated between two porphyrin rings. The metal–nitrogen bonds thus formed are weak and the products could not be purified due to decomposition in air. Partial decomposition is also shown by the molecular weight and analytical results. It is of interest that the reaction of I with neutral copper acetate (2:1 mole ratio) in a basic solvent at room temperature for 5 hr results in the replacement of the rhenium–carbonyl moiety by cupric ion to form a square planar copper(II) porphyrin complex.

By reaction of I with ditechnetium decacarbonyl, $Tc_2(CO)_{10}$, in 1 to 0.6 mole ratio in refluxing decalin under

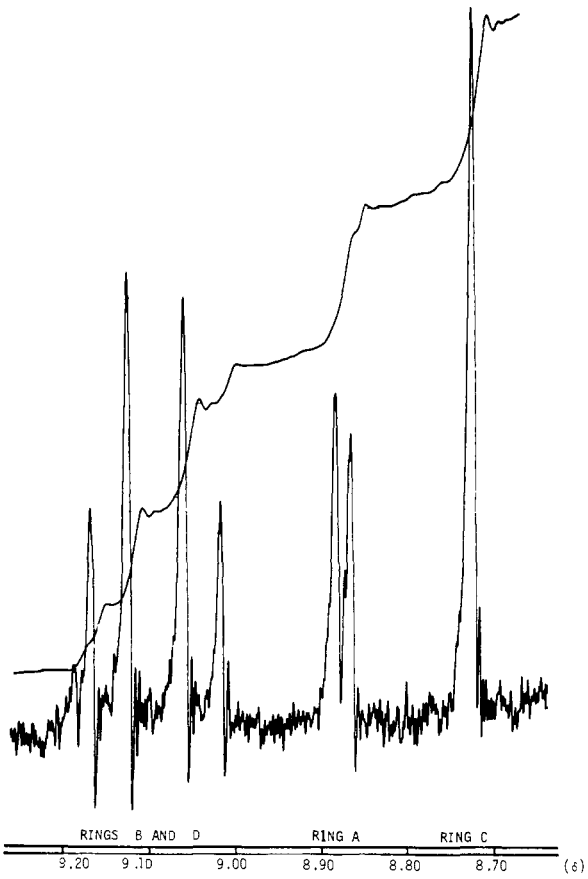

Figure 1. HA-100 NMR spectrum for the pyrrole protons in compound II.

Table III. Visible Absorptions for (H-MP)Re(CO)$_3$ (I) and Its Unstable Derivatives

Derivatives	λ_{max} (in acetone), nm
(H-MP)Re(CO)$_3$ (I)	400 (Soret), 480, 580
I + CH_3COOAg	387 (Soret), 480, 560, 580
I + $(CH_3COO)_2Hg$	385 (Soret), 480, 530, 570, 580
I + $(CH_3COO)_2Pb\cdot 3H_2O$	388 (Soret), 460, 580
I + $(CH_3COO)_2Cu\cdot H_2O$	395 (Soret), 520, 560[a]

[a] This is the visible absorption of Cu^{II}MPIXDME.

argon, an unusual heterodinuclear metalloporphyrin complex, μ-[mesoporphyrin IX dimethyl esterato]-[tricarbonylrhenium(I)][tricarbonyltechneum(I)], $(OC)_3TcMPRe(CO)_3$ (V), was prepared.[45] This new complex was also characterized by elemental analyses, molecular weight determination, visible absorption, infrared, ^1H NMR, and mass spectra. Except for small shifts, the visible absorption spectrum of V in methylene chloride resembles that of III. Because of the similarities in physical and chemical properties among III, IV, and V, structures identical with that of IV were proposed for III and V as shown in Figure 4.

Fluxional Behavior. Due to its more highly symmetric porphyrin (Figure 2c), the ^1H NMR spectrum of II is much simpler than that of I. At room temperature the ^1H NMR spectrum showed the nonequivalence of the β-pyrrole protons in II (Figure 1) and also the bridged methine protons in I. Temperature dependent ^1H NMR spectral changes for I and II dissolved in 1,1,2,2-tetrachloroethane (bp 146°) are shown in Figure 5. As the temperature is raised, the peaks broaden, coalesce, and gradually sharpen. The changes have all been shown to be completely reversible with temperature. These results illustrate that both I and II display a fluxional character.[49] This is best explained in terms of an intramolecular rearrangement of the rhenium-

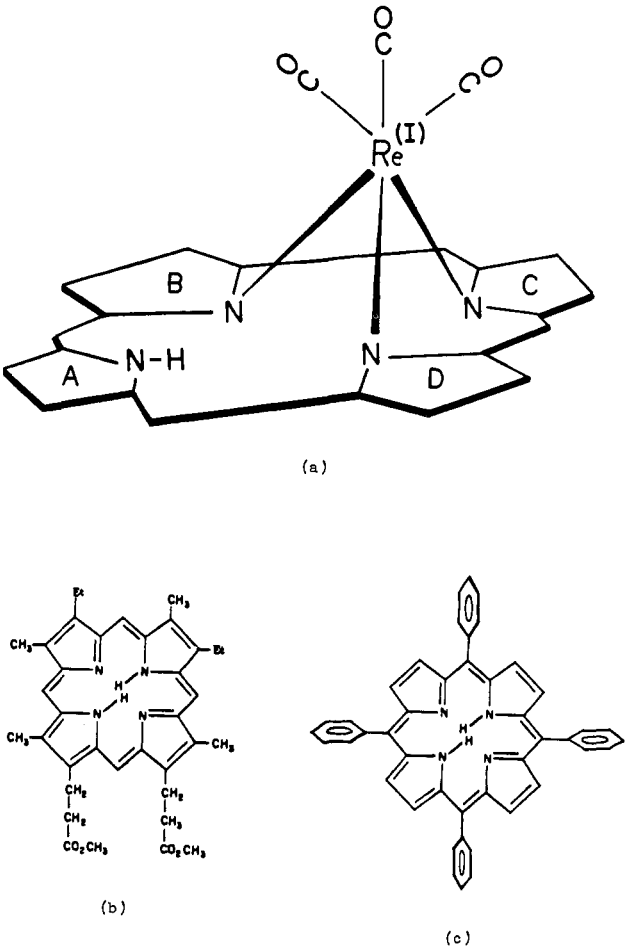

Figure 2. (a) Proposed structure for HTPPRe(CO)$_3$ and HMPRe(CO)$_3$ (phenyl and alkyl substituents are left out of the porphine ring for clarity); (b) mesoporphyrin IX dimethyl ester, H_2MP; (c) *meso*-tetraphenylporphine, H_2TPP.

carbonyl group among the four ring nitrogens of porphyrin and a concomitant movement of the N-H proton. It can also be regarded as an intramolecular substitution at rhenium. A solution containing I and excess $H_2MPIXDME$ showed no broadening of the free ligand bridged methine proton peak in the fast exchange region for I. Further, the coalescence temperatures were not shifted by changes in the concentrations of the complexes within the standard deviations of the experiment (ca. ±5°). These results show that the thermal rearrangement process is intramolecular rather than intermolecular. Also, the occurence of either dissociation and recombination of the metal-carbonyl moiety and the porphyrin ligand or interchange of ligands between two molecules at high temperature is ruled out by the failure of attempts to convert III to I by reflux in decalin with excess porphyrin.

Unusual Technetium Metalloporphyrin Complexes. By reflux of $Tc_2(CO)_{10}$ and porphyrin in decalin, in a manner similar to that used in preparing the rhenium complexes, several technetium porphyrins were prepared. Depending on the porphyrin used and the ratios of reactants, the following compounds were prepared: (monohydrogen mesoporphyrin IX dimethyl esterato)tricarbonyltechnetium(I), $HMPTc(CO)_3$ (VI); μ-[mesoporphyrin IX dimethyl esterato]-bis[tricarbonyltechnetium(I)], $MP[Tc(CO)_3]_2$ (VII); and μ-[*meso*-tetraphenylporphinato]-bis[tricarbonyltechnetium(I)], $TPP[Tc(CO)_3]_2$ (VIII).

These compounds are considered to be structurally similar to the corresponding rhenium complexes. A single-crys-

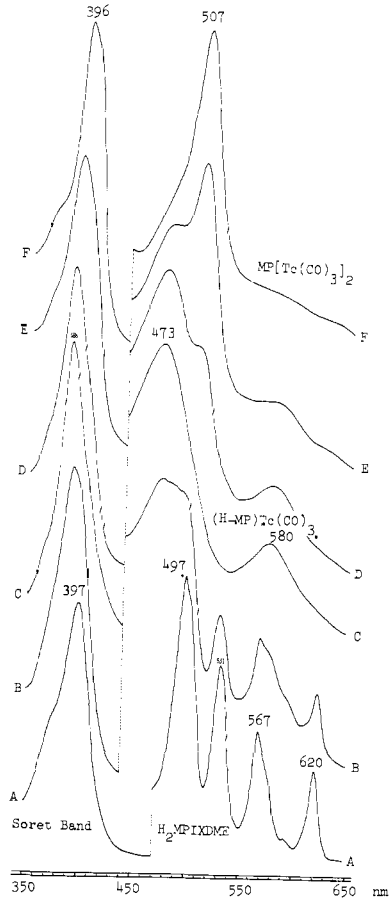

Figure 3. Repeated scan spectrophotometry shows progress of the formation of $(H\text{-}MP)Tc(CO)_3$ and $MP[Tc(CO)_3]_2$.

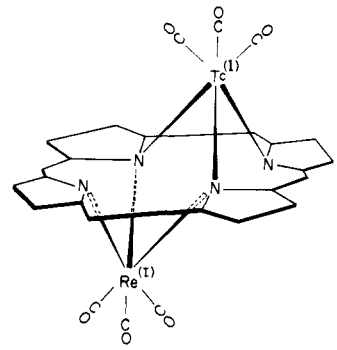

Figure 4. Schematic diagram of $(OC)_3ReMpTc(CO)_3$, V; the alkyl substituents on the porphine ring were omitted for clarity.

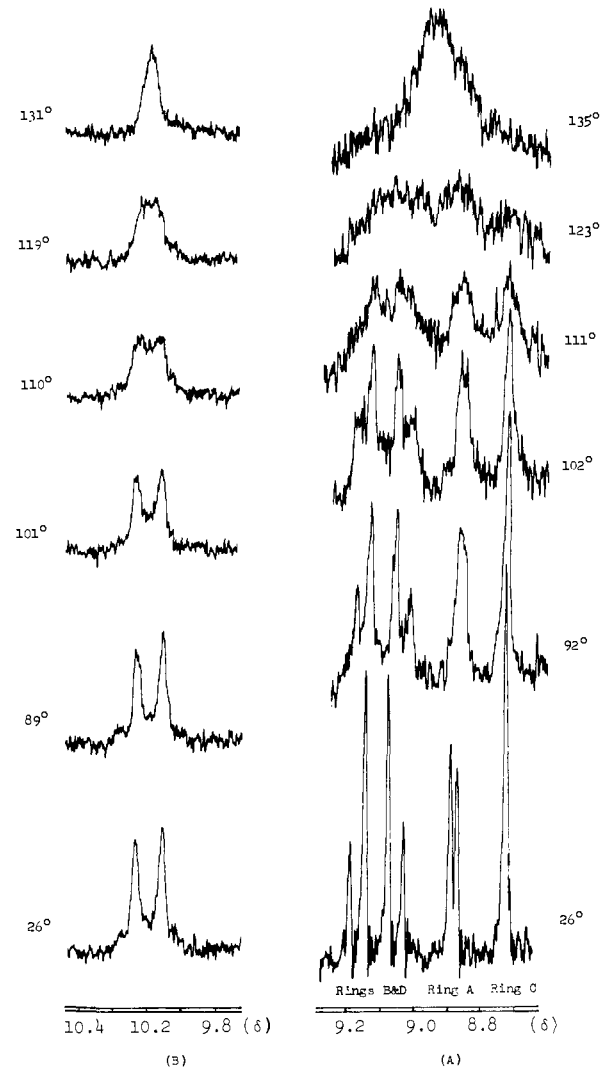

Figure 5. The 100-MHz variable temperature ^1H NMR spectra for (A) β-pyrrole protons of $HTPPRe(CO)_3$ and (B) bridge methine protons of $HMPTc(CO)_3$ (both in $C_2H_2Cl_4$ and temperature in °C).

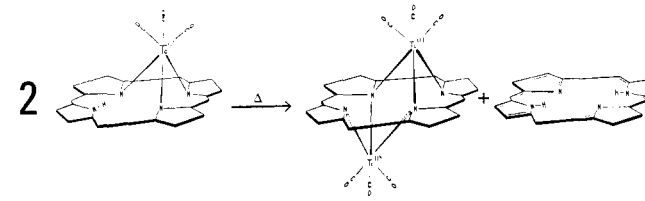

Figure 6. Disproportionating of $(H\text{-}MP)Tc(CO)_3$ by heating.

tal X-ray diffraction analysis of VIII, reported here, has confirmed the similarity.

The reaction of $H_2MPIXDME$ and $Tc_2(CO)_{10}$ in a mole ratio of 1 to 0.6 was used to give the monotechnetium complex, VI. However, when the same reaction was run for longer periods of time; the products were the free porphyrin and μ-[mesoporphyrin IX dimethyl esterato]-bis[tricarbonyltechnetium(I)], $MP[Tc(CO)_3]_2$ (VII). The results of these two reactions suggest that $H_2MPIXDME$ and $Tc_2(CO)_{10}$ react initially to form $(H\text{-}MP)Tc(CO)_3$ which then disproportionates (Figure 6) into $MP[Tc(CO)_3]_2$ and $H_2MPIXDME$. This behavior was confirmed by heating a benzene–dichloromethane (50/50) solution of a purified sample of VI to dryness in a hot water bath at 50–60°. Chromatography on a talc column showed the presence of both $H_2MPIXDME$ and VII.

Complex VII was stable at room temperature but it was thermally unstable in refluxing decalin in a different manner than complex VI. When a decalin solution of VII was refluxed under argon for more than 4 hr, a large amount of solid material precipitated from the decalin. The unknown solid compound (IX) was insoluble in most organic solvents but was slightly soluble in methylene chloride. The visible spectrum of the solution had a sharp absorption at 358 nm and three weak, broad peaks at 397 (Soret), 500, and 540 nm. The unknown compound turned black above 260° without melting. The infrared spectrum of IX in the solid phase (KBr) also showed two strong metal–carbonyl stretches at 2044 and 1925 cm^{-1} and a split ester carbonyl peak centered at 1725 cm^{-1}. A similar splitting of an ester carbonyl peak has been observed in the solid ruthenium metalloporphyrin complex, MPRuCO, and tentatively assigned to coordination between the ester carbonyl and the metal.[50] The unknown solid, IX, may be a coordination polymer[51,52] involving similar coordination between a metal and an ester carbonyl.

Table IV. Crystal Data and Experimental Conditions

	$TPP[Re(CO)_3]_2$	$TPP[Tc(CO)_3]_2$
a, Å	11.887 (2)	11.934 (1)
b, Å	16.363 (2)	16.295 (1)
c, Å	11.586 (2)	11.596 (1)
β, deg	117.02 (1)	117.02 (1)
Volume, Å^3	2008	2009
Room temp, °C	21	18
d_{calcd}, g/cm^3	1.908	1.619
d_{measd}, g/cm^3	1.90	1.60
Mol wt, daltons	1153.2 ($C_{50}H_{28}O_6N_4Re_2$)	978.8 ($C_{50}H_{28}O_6N_4Tc_2$)
Z	2	2
Space group	$P2_1/c$	$P2_1/c$
μ(Mo Kα radiation), cm^{-1}	64.4	7.37
Systematic absences	$h0l$(l odd); $0k0$(k odd)	same
Scan rate	1°/min if peak height ≥3 counts/sec 2°/min if peak height <3 counts/sec	4°/min if $2\theta \leq 30°$ 2°/min if $2\theta > 30°$
Scan range	1.50°	2.25°
Max sin θ/λ	0.65 (27.5 in θ)	0.703 (30° in θ)
Total refln	4769	6013
Refln with $I \geq 3\sigma_I$	2385	3762
Coincidence factor, τ	4.31×10^{-7} counts^{-1}	5.50×10^{-7} counts^{-1}
Stability constant K	0.03	0.015
$R = \Sigma\|\|F_o\| - \|F_c\|\|/\Sigma\|F_o\|$	0.045	0.032
$R_w = \Sigma w\|\|F_o\| - \|F_c\|^2/\Sigma wF_o^2)^{1/2}$	0.044	0.027
SEF = $(\Sigma\|\|F_o\| - \|F_c\|^2/N_{obsd} - N_{var})^{1/2}$	1.33	1.37

Table V. Fractional Coordinates and Thermal Motion Parameters Derived from the Least-Squares Refinement[a] for $TPP[Tc(CO)_3]_2$

Atom	X	Y	Z	U(11)	U(22)	U(33)	U(12)	U(13)	U(23)
Tc	−0.0901 (1)	0.0515 (1)	0.0342 (1)	301 (1)	238 (1)	270 (1)	7 (1)	156 (0)	19 (1)
N(1)	−0.0644 (2)	−0.0656 (1)	0.1304 (2)	292 (12)	270 (13)	238 (10)	−23 (10)	131 (9)	−3 (9)
N(2)	0.1345 (2)	0.0425 (1)	0.1422 (2)	294 (12)	281 (13)	222 (10)	−33 (10)	110 (9)	8 (10)
C(1)	−0.1464 (2)	−0.1293 (1)	0.0877 (2)	269 (14)	282 (14)	289 (13)	−22 (11)	145 (12)	16 (11)
C(2)	−0.1234 (2)	−0.1837 (1)	0.1943 (2)	350 (17)	298 (16)	332 (15)	−37 (13)	170 (13)	40 (12)
C(3)	−0.0260 (3)	−0.1523 (2)	0.2988 (3)	336 (16)	359 (16)	290 (15)	10 (14)	132 (13)	82 (13)
C(4)	0.0142 (2)	−0.0796 (1)	0.2578 (2)	301 (15)	302 (14)	261 (13)	8 (12)	137 (12)	25 (11)
C(5)	0.1226 (2)	−0.0340 (1)	0.3278 (2)	304 (15)	313 (16)	230 (12)	14 (11)	113 (11)	18 (11)
C(6)	0.1774 (2)	0.0195 (1)	0.2735 (2)	290 (15)	368 (15)	244 (13)	−45 (12)	115 (12)	−18 (12)
C(7)	0.2917 (3)	0.0603 (2)	0.3509 (2)	393 (17)	598 (23)	230 (13)	−195 (18)	79 (13)	−21 (16)
C(8)	0.3207 (3)	0.1082 (2)	0.2745 (3)	340 (18)	577 (23)	289 (15)	−196 (17)	78 (14)	−21 (15)
C(9)	0.2253 (2)	0.0993 (1)	0.1452 (2)	302 (16)	334 (16)	289 (14)	−73 (13)	127 (12)	−32 (12)
C(10)	0.2300 (2)	0.1412 (1)	0.0421 (2)	301 (15)	275 (14)	283 (13)	−53 (12)	137 (12)	−4 (11)
C(11)	0.1914 (2)	−0.0473 (2)	0.4713 (2)	285 (13)	384 (15)	225 (12)	−53 (15)	109 (10)	22 (13)
C(12)	0.2651 (3)	−0.1159 (2)	0.5221 (3)	440 (20)	527 (22)	322 (17)	88 (17)	187 (15)	33 (16)
C(13)	0.3327 (3)	−0.1270 (2)	0.6547 (3)	439 (22)	683 (27)	415 (20)	203 (20)	180 (17)	208 (19)
C(14)	0.3245 (3)	−0.0693 (2)	0.7363 (3)	446 (20)	855 (33)	253 (15)	53 (20)	143 (15)	125 (18)
C(15)	0.2486 (3)	−0.0024 (2)	0.6880 (3)	600 (25)	629 (26)	290 (17)	12 (20)	201 (17)	−55 (17)
C(16)	0.1812 (3)	0.0086 (2)	0.5549 (3)	509 (22)	451 (20)	317 (16)	61 (17)	159 (16)	15 (15)
C(17)	0.3318 (2)	0.2038 (1)	0.0716 (2)	301 (15)	343 (16)	267 (14)	−70 (13)	108 (12)	13 (12)
C(18)	0.4160 (3)	0.1936 (2)	0.0204 (3)	373 (17)	394 (17)	363 (17)	−35 (15)	190 (14)	−1 (15)
C(19)	0.5105 (3)	0.2504 (2)	0.0469 (3)	320 (18)	578 (24)	481 (20)	−72 (17)	186 (16)	69 (18)
C(20)	0.5219 (3)	0.3172 (2)	0.1222 (3)	340 (19)	477 (22)	510 (21)	−147 (17)	116 (17)	41 (17)
C(21)	0.4378 (3)	0.3290 (2)	0.1711 (3)	509 (22)	360 (20)	506 (21)	−130 (17)	181 (18)	−88 (16)
C(22)	0.3434 (3)	0.2726 (2)	0.1453 (3)	407 (20)	457 (21)	453 (20)	−109 (16)	232 (17)	−96 (16)
C(23)	−0.1080 (3)	0.1523 (2)	−0.0568 (3)	507 (21)	379 (18)	543 (21)	50 (16)	335 (18)	71 (16)
C(24)	−0.2652 (2)	0.0557 (2)	−0.0249 (2)	383 (17)	410 (17)	302 (14)	65 (17)	163 (13)	30 (15)
C(25)	−0.0697 (3)	0.1138 (2)	0.1793 (3)	464 (20)	298 (16)	543 (20)	−43 (15)	312 (17)	−63 (15)
O(1)	−0.1236 (3)	0.2137 (1)	−0.1099 (3)	1080 (26)	458 (17)	1072 (24)	263 (17)	734 (22)	374 (17)
O(2)	−0.3711 (2)	0.0604 (1)	−0.0570 (2)	336 (13)	916 (22)	569 (15)	121 (15)	178 (11)	57 (16)
O(3)	−0.0576 (2)	0.1511 (1)	0.2682 (2)	909 (23)	598 (18)	737 (19)	−149 (16)	502 (18)	−326 (15)
H(1)	−0.165 (3)	−0.233 (1)	0.186 (2)	29 (7)					
H(2)	0.007 (3)	−0.175 (2)	0.374 (3)	34 (8)					
H(3)	0.335 (2)	0.055 (2)	0.434 (3)	32 (6)					
H(4)	0.389 (2)	0.138 (1)	0.298 (2)	25 (6)					
H(5)	0.268 (3)	−0.149 (2)	0.471 (3)	33 (8)					
H(6)	0.382 (3)	−0.177 (2)	0.691 (3)	38 (7)					
H(7)	0.366 (3)	−0.078 (1)	0.820 (3)	36 (7)					
H(8)	0.245 (3)	0.034 (2)	0.738 (3)	41 (9)					
H(9)	0.135 (2)	0.056 (2)	0.522 (2)	33 (7)					
H(10)	0.415 (3)	0.145 (2)	−0.022 (3)	39 (8)					
H(11)	0.563 (3)	0.238 (2)	0.016 (3)	45 (10)					
H(12)	0.583 (3)	0.353 (2)	0.137 (3)	47 (9)					
H(13)	0.438 (2)	0.373 (2)	0.210 (2)	26 (7)					
H(14)	0.295 (3)	0.280 (2)	0.182 (3)	34 (8)					

[a] In this and subsequent tables estimated standard deviations for the least significant figure are in parentheses. The Debye–Waller factor is defined as: $T = \exp[-2\pi^2\Sigma_i\Sigma_j a_i a_j h_i h_j U_{ij}]$. The values for U have been multiplied by 10^4. Isotropic B's for hydrogen atoms defined by: $\exp[-B(\sin^2\theta)/\lambda^2]$ are given in the column labeled U_{11}. These have been multiplied by 10.

Table VI. Fractional Coordinates and Thermal Motion Parameters Derived from the Least-Squares Refinement for $TPP[Re(CO)_3]_2$[a]

Atom	X	Y	Z	U(11)	U(22)	U(33)	U(12)	U(13)	U(23)
Re	−0.0910 (1)	0.0515 (1)	0.0351 (1)	344 (2)	299 (2)	313 (2)	8 (3)	169 (1)	22 (3)
N(1)	−0.0645 (9)	−0.0657 (5)	0.1314 (9)	410 (57)	264 (58)	270 (48)	−38 (45)	161 (47)	41 (45)
N(2)	0.1334 (8)	0.0416 (6)	0.1408 (8)	309 (53)	368 (61)	281 (51)	−143 (50)	157 (45)	−45 (52)
C(1)	−0.1469 (10)	−0.1307 (7)	0.0889 (11)	213 (57)	353 (69)	434 (72)	43 (53)	219 (58)	59 (59)
C(2)	−0.1226 (11)	−0.1814 (6)	0.1977 (11)	405 (74)	254 (61)	335 (69)	−44 (56)	212 (63)	75 (53)
C(3)	−0.0234 (10)	−0.1516 (7)	0.3014 (11)	356 (72)	383 (71)	372 (72)	−7 (60)	213 (63)	5 (62)
C(4)	0.0149 (12)	−0.0796 (7)	0.2604 (11)	439 (78)	481 (80)	240 (63)	−41 (61)	227 (62)	114 (56)
C(5)	0.1215 (10)	−0.0343 (6)	0.3281 (10)	322 (65)	298 (71)	212 (56)	−5 (51)	65 (52)	33 (48)
C(6)	0.1758 (11)	0.0196 (8)	0.2710 (13)	352 (75)	493 (78)	471 (82)	−15 (63)	235 (69)	−83 (67)
C(7)	0.2897 (11)	0.0596 (9)	0.3482 (11)	412 (71)	584 (86)	349 (68)	−33 (77)	168 (60)	59 (77)
C(8)	0.3181 (12)	0.1070 (7)	0.2704 (11)	452 (80)	520 (81)	274 (66)	−220 (66)	191 (63)	17 (62)
C(9)	0.2250 (11)	0.0990 (7)	0.1432 (10)	379 (72)	393 (70)	196 (58)	10 (58)	155 (57)	−35 (55)
C(10)	0.2313 (10)	0.1406 (6)	0.0416 (10)	311 (65)	260 (63)	283 (64)	62 (54)	132 (56)	1 (54)
C(11)	0.1916 (9)	−0.0457 (8)	0.4712 (10)	299 (56)	516 (71)	345 (60)	−75 (66)	191 (50)	−47 (71)
C(12)	0.2670 (13)	−0.1160 (8)	0.5245 (13)	498 (89)	522 (84)	513 (86)	144 (71)	271 (77)	−32 (72)
C(13)	0.3318 (13)	−0.1248 (9)	0.6557 (13)	537 (96)	755 (112)	357 (83)	342 (86)	186 (78)	225 (82)
C(14)	0.3243 (14)	−0.0665 (10)	0.7351 (12)	645 (101)	863 (131)	337 (79)	−129 (93)	236 (78)	94 (86)
C(15)	0.2497 (14)	−0.0023 (9)	0.6891 (12)	753 (113)	699 (105)	226 (65)	105 (87)	213 (74)	−17 (71)
C(16)	0.1828 (13)	0.0089 (8)	0.5564 (13)	635 (93)	410 (75)	448 (81)	86 (69)	258 (74)	31 (68)
C(17)	0.3341 (11)	0.2029 (7)	0.0711 (11)	356 (71)	436 (77)	303 (69)	−143 (60)	108 (60)	−126 (59)
C(18)	0.4175 (12)	0.1936 (7)	0.0218 (12)	455 (77)	400 (65)	418 (77)	−66 (65)	284 (66)	0 (64)
C(19)	0.5125 (12)	0.2508 (9)	0.0473 (13)	492 (80)	576 (88)	567 (90)	−78 (79)	383 (76)	74 (80)
C(20)	0.5221 (13)	0.3169 (8)	0.1244 (14)	440 (91)	515 (86)	593 (103)	−196 (73)	143 (83)	92 (76)
C(21)	0.4376 (13)	0.3278 (8)	0.1697 (13)	568 (94)	377 (75)	514 (89)	−143 (68)	276 (79)	−130 (68)
C(22)	0.3444 (12)	0.2707 (8)	0.1437 (13)	485 (84)	466 (86)	579 (90)	−141 (70)	342 (77)	−33 (75)
C(23)	−0.1059 (13)	0.1497 (9)	−0.0530 (14)	648 (101)	554 (96)	602 (102)	165 (85)	483 (89)	−23 (87)
C(24)	−0.2641 (13)	0.0555 (8)	−0.0223 (11)	745 (98)	344 (67)	277 (65)	145 (90)	269 (69)	24 (74)
C(25)	−0.0687 (13)	0.1120 (10)	0.1785 (16)	413 (93)	697 (111)	802 (125)	−105 (80)	343 (95)	213 (98)
O(1)	−0.1213 (11)	0.2112 (6)	−0.1077 (12)	1098 (103)	577 (75)	1299 (112)	259 (71)	866 (94)	345 (76)
O(2)	−0.3718 (9)	0.0595 (7)	−0.0568 (9)	475 (60)	1075 (92)	532 (64)	264 (73)	188 (53)	119 (74)
O(3)	−0.0564 (11)	0.1516 (7)	0.2678 (10)	1011 (94)	680 (78)	764 (83)	−101 (71)	571 (78)	−315 (69)

[a] See footnote *a* in Table V. Hydrogen atom positions were assumed to be in their theoretically calculated positions. They are not listed here.

Table VII. Root-Mean-Square Amplitudes of Vibration (in A) along Principal Axes of Thermal Ellipsoids

	$TPP[Re(CO)_3]_2$			$TPP[Tc(CO)_3]_2$		
	Axis 1	Axis 2	Axis 3	Axis 1	Axis 2	Axis 3
M	0.165 (2)	0.176 (2)	0.188 (1)	0.148 (1)	0.158 (1)	0.176 (1)
N(1)	0.14 (3)	0.18 (2)	0.21 (2)	0.150 (6)	0.160 (4)	0.175 (4)
N(2)	0.13 (3)	0.16 (2)	0.22 (2)	0.147 (5)	0.159 (4)	0.183 (5)
C(1)	0.11 (5)	0.18 (2)	0.22 (2)	0.148 (9)	0.171 (3)	0.175 (6)
C(2)	0.12 (4)	0.19 (2)	0.20 (2)	0.152 (8)	0.187 (3)	0.196 (7)
C(3)	0.17 (4)	0.20 (2)	0.20 (1)	0.153 (6)	0.185 (5)	0.206 (5)
C(4)	0.10 (6)	0.21 (2)	0.23 (2)	0.155 (7)	0.172 (6)	0.178 (4)
C(5)	0.14 (2)	0.17 (2)	0.20 (3)	0.150 (5)	0.175 (6)	0.180 (5)
C(6)	0.17 (4)	0.20 (2)	0.24 (2)	0.156 (4)	0.167 (7)	0.198 (4)
C(7)	0.18 (3)	0.20 (2)	0.25 (2)	0.148 (4)	0.181 (9)	0.274 (5)
C(8)	0.13 (5)	0.18 (2)	0.27 (2)	0.148 (6)	0.185 (8)	0.268 (5)
C(9)	0.13 (4)	0.19 (2)	0.20 (2)	0.156 (5)	0.173 (7)	0.198 (5)
C(10)	0.15 (3)	0.17 (2)	0.19 (2)	0.151 (7)	0.168 (5)	0.186 (5)
C(11)	0.15 (4)	0.18 (2)	0.23 (2)	0.147 (6)	0.161 (5)	0.206 (5)
C(12)	0.17 (4)	0.23 (2)	0.26 (2)	0.174 (7)	0.197 (6)	0.242 (5)
C(13)	0.15 (3)	0.21 (4)	0.32 (2)	0.165 (6)	0.213 (10)	0.287 (5)
C(14)	0.16 (4)	0.24 (2)	0.31 (2)	0.150 (6)	0.216 (7)	0.297 (6)
C(15)	0.14 (3)	0.25 (2)	0.30 (2)	0.161 (7)	0.245 (6)	0.257 (6)
C(16)	0.20 (2)	0.21 (3)	0.26 (2)	0.178 (5)	0.205 (6)	0.240 (6)
C(17)	0.14 (2)	0.20 (4)	0.23 (2)	0.157 (6)	0.163 (4)	0.206 (6)
C(18)	0.16 (5)	0.20 (2)	0.23 (2)	0.177 (10)	0.192 (4)	0.205 (5)
C(19)	0.14 (6)	0.25 (2)	0.25 (2)	0.164 (9)	0.212 (5)	0.256 (6)
C(20)	0.16 (4)	0.22 (2)	0.30 (3)	0.156 (8)	0.214 (5)	0.267 (7)
C(21)	0.17 (2)	0.22 (4)	0.26 (2)	0.165 (6)	0.234 (5)	0.247 (8)
C(22)	0.16 (5)	0.22 (3)	0.26 (3)	0.179 (7)	0.195 (9)	0.240 (4)
C(23)	0.13 (7)	0.24 (2)	0.28 (2)	0.184 (10)	0.192 (7)	0.248 (4)
C(24)	0.15 (4)	0.17 (2)	0.28 (2)	0.170 (6)	0.182 (7)	0.216 (5)
C(25)	0.15 (6)	0.25 (2)	0.32 (2)	0.168 (5)	0.185 (11)	0.242 (3)
O(1)	0.21 (2)	0.25 (4)	0.40 (1)	0.167 (6)	0.256 (10)	0.374 (3)
O(2)	0.19 (2)	0.24 (2)	0.34 (1)	0.176 (4)	0.246 (5)	0.307 (4)
O(3)	0.18 (4)	0.28 (2)	0.34 (1)	0.174 (8)	0.269 (7)	0.328 (3)

The elemental analyses results and all of the spectra data for both rhenium and technetium metalloporphyrin complexes, I–IX, are summarized in Tables I and II.

X-Ray Structural Data. A preliminary study on the single-crystal X-ray diffraction analysis of $TPP[Re(CO)_3]_2$, IV, has already been reported.[44] This structure has now been fully refined. In addition, the structure of the analogous technetium complex $TPP[Tc(CO)_3]_2$, VIII, has been determined and is reported here. Results of the analysis are tabulated in Tables IV–X. Within standard deviations the

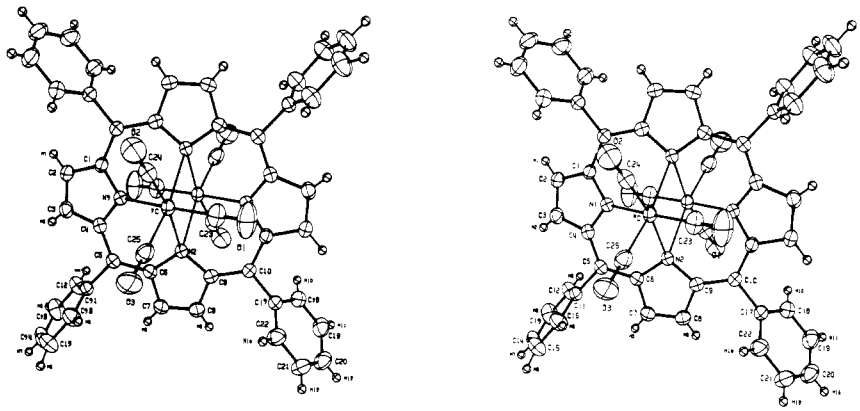

Figure 7. A stereoview of the structure of μ-[*meso*-tetraphenylporphinato]-bis[tricarbonyltechnetium(I)]. Atoms not labeled are centrosymmetrically related. The thermal ellipsoids are drawn for 50% probability, except those of the hydrogen atoms which are not drawn to scale.

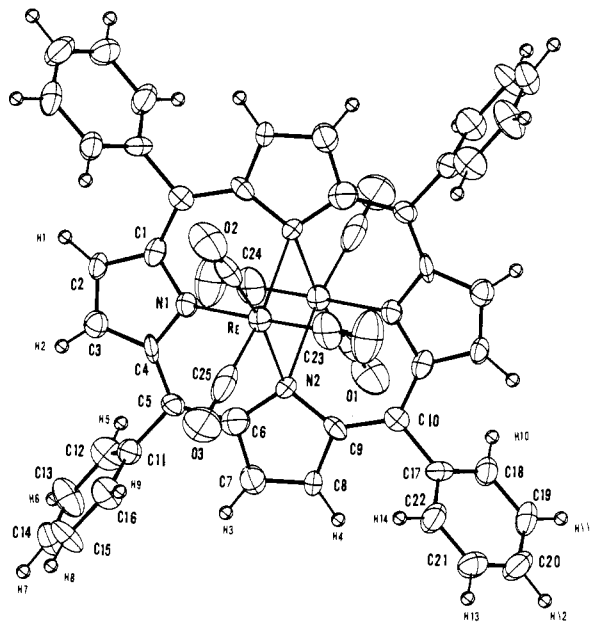

Figure 8. The structure of μ-[*meso*-tetraphenylporphinato]-bis[tricarbonylrhenium(I)]. The number scheme used is shown. Atoms not labeled are centrosymmetrically related. The thermal ellipsoids are drawn for 50% probability, except for those of the hydrogen atoms which are not drawn to scale.

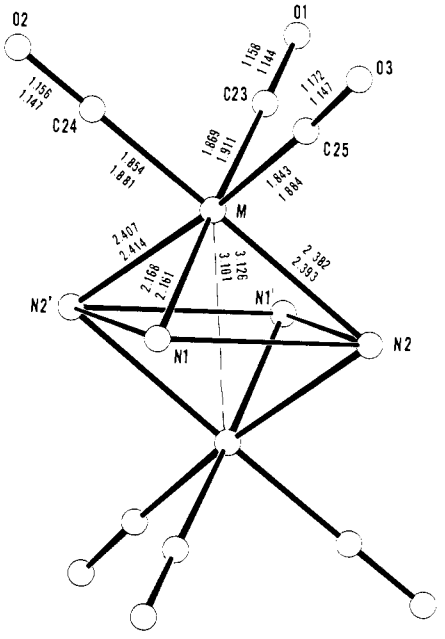

Figure 9. Coordination sphere showing bond distances around the metal atoms in $TPP[Re(CO)_3]_2$ (top value) and $TPP[Tc(CO)_3]_2$ (lower value). The lines between nitrogens signify the plane of the macrocycle. Primed atoms or atoms not labeled are centrosymmetrically related to unprimed atoms.

two compounds are virtually isostructural. Both are centrosymmetric complexes having two metal ions bonded to the porphyrin, one above and one below the plane of the macrocyclic ligand. A comparison of these two complexes of group 7B congeners is of interest.

The X-ray data obtained for the technetium complex are superior to those obtained for the rhenium complex. Absorption effects are much smaller in the former, and the metal ion contributes to a smaller percentage of the scattering power, which means the nonmetal ions can be located with more accuracy. In addition, data could be collected to a higher sin θ/λ limit in the technetium case, and a higher percentage of the reflections could be observed. As a result of this increased accuracy more may be said about the structural details in the technetium complex. While the same details are also noted in $TPP[Re(CO)_3]_2$, the significance of these is harder to judge because of the lower accuracy. In the subsequent discussion, the value found in $TPP[Tc(CO)_3]_2$ is used unless otherwise specified. Bond lengths and angles for both complexes are listed in Tables VIII and IX.

A stereoview of $TPP[Tc(CO)_3]_2$ is shown in Figure 7. For comparison the structure of $TPP[Re(CO)_3]_2$ is shown in Figure 8. Figure 9 shows the coordination sphere and the bond lengths involving the metal atom in both complexes. In each case the metal atoms are situated 1.42 Å from the plane defined by the four pyrrole nitrogen atoms. The metal ions are not positioned directly over the center of the macrocycle but are set to one side such that each metal ion is bonded to three nitrogen atoms. N(2) is bonded to both metal ions. The distances from the metal ion to the fourth nitrogen atom are 3.230 and 3.208 Å for the rhenium and technetium complexes, respectively. The M-N(1) distance is 2.16 Å in both cases. The two M-N(2) bonds are much longer, averaging 2.39 Å in both complexes. The M-C bond lengths appear to be normal. There is a small but significant difference in the M-M distances, with the Tc-Tc distance (3.101 (1)) Å being 0.02 Å shorter that the Re-Re distance (3.126 (1) Å). This small difference in the covalent radii of congeners in the second- and third-row transition metal series can be attributed to the lanthanide contraction effect.

The porphyrin macrocycle is highly distorted. The distortion is such that if one considers the mean plane of the macrocycle, pyrrole ring 1 (N(1), C(1)-C(4)) is "bent" toward the metal atom to which it is coordinated while pyrrole ring 2 (N(2), C(6)-C(9)) lies almost in the mean plane

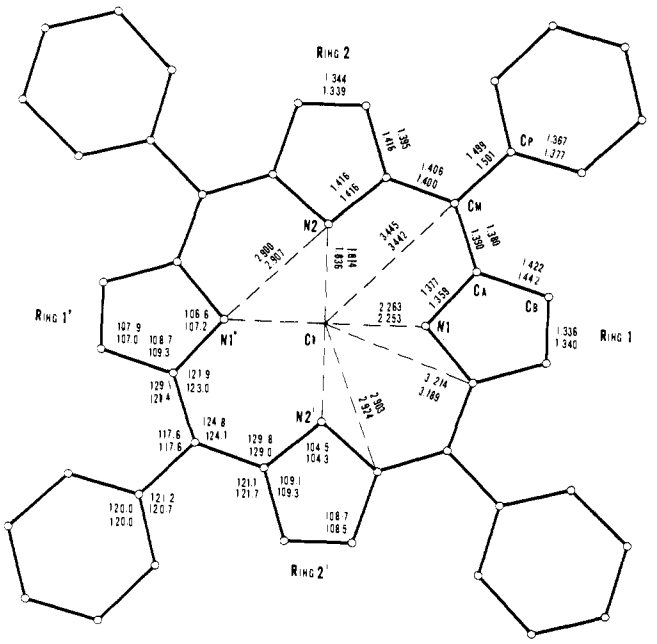

Figure 10. Schematic drawing of the macrocycle showing averaged bond lengths in angstroms and angles in degrees as found in TPP[Re(CO)$_3$]$_2$ (top value) and TPP[Tc(CO)$_3$]$_2$ (lower value). Also shown is the notation for different types of carbon atoms.

of the macrocycle. The individual pyrrole rings are quite planar, but the angle between the least-squares planes of the two adjacent rings is 17.0° in both complexes. Another measure of the bending is the perpendicular distance of an atom in one pyrrole ring from the least-squares plane defined by the equivalent ring across the macrocycle. Thus, N(1)′ lies 1.83 Å from the plane of pyrrole ring 1. N(2)′ lies 0.34 Å from the plane of pyrrole ring 2. (The primes indicate an atom related by a center of symmetry.) Table X lists various least-squares planes of interest and the interplanar angles for the two complexes, TPP[Tc(CO)$_3$]$_2$ and TPP[Re(CO)$_3$]$_2$.

The distortion of the macrocycle leads to unusual distances between opposite pyrrole nitrogen atoms. The optimum value for the diameter of the "hole" of an undistorted metalloporphyrin complex has been estimated[53] to be 4.02 Å. The N(1)-N(1)′ distance is unusually long (4.506 (3) Å in TPP[Tc(CO)$_3$]$_2$). It is caused by the large deviation of pyrrole ring from the mean plane of the macrocycle. The N(2)-(2)′ distance is unusually short (3.672 (4) Å in the ditechnetium complex). This shortening apparently arises so that octahedral coordination may be attained. It is of interest to note that the two Cm-Cm distances are approximately the same and similar to those found in monometallic porphyrin complexes.[53]

Figure 10 shows a schematic drawing of the macrocycle and the averaged bond lengths and angles. Because pyrrole rings 1 and 2 are not chemically equivalent, they must be considered separately in the averages. Also shown in Figure 10 is the nomenclature used for the different type of carbon atoms.

The involvement of N(2) in two coordination bonds might be expected to affect the double bond character of the Cα-N(2) bonds. This effect is indeed seen, as the average Cα-N(2) distance is 1.416 (3) Å as compared to the Cα-N(1) distance of 1.359 (4) Å. The latter distance is typical of that found in normal metalloporphyrin complexes.[53] In addition, the C(6)-N(2)-(9) angle is 2.9° less than the C(1)-N(1)-C(4) angle.

To a lesser extent the bond lengths and angles around Cα atoms on pyrrole ring 2 are affected. The average Cα-Cβ

Table VIII. Bond Lengths (Å) in TPP[Re(CO)$_3$]$_2$ and TPP[Tc(CO)$_3$]$_2$[a,b]

Type	TPP[Re(CO)$_3$]$_2$		TPP[Tc(CO)$_3$]$_2$	
M–N(1)	2.168 (9)		2.161 (2)	
M–N(2)	2.382 (9)		2.393 (2)	
M–N(2)′[c]	2.407 (10)		2.414 (2)	
M–C(23)	1.869 (16)		1.911 (4)	
M–C(24)	1.854 (16)	1.855 (13)	1.881 (4)	1.892 (17)
M–C(25)	1.847 (19)		1.884 (4)	
N(1)–C(1)	1.377 (15)	1.377 (1)	1.356 (4)	1.359 (4)
N(1)–C(4)	1.376 (14)		1.362 (3)	
C(1)–C(2)	1.424 (18)	1.422 (3)	1.444 (5)	1.442 (4)
C(3)–C(4)	1.420 (20)		1.439 (5)	
C(1)–C(10)′[c]	1.392 (15)	1.380 (17)	1.391 (4)	1.390 (2)
C(4)–C(5)	1.367 (16)		1.389 (4)	
C(2)–C(3)	1.336 (14)		1.342 (4)	
N(2)–C(6)	1.403 (18)	1.416 (17)	1.418 (4)	1.416 (3)
N(2)–C(9)	1.428 (17)		1.414 (5)	
C(6)–C(7)	1.400 (17)	1.395 (7)	1.412 (4)	1.416 (5)
C(8)–C(9)	1.390 (14)		1.419 (4)	
C(5)–C(6)	1.422 (21)	1.406 (22)	1.400 (5)	1.400 (1)
C(9)–C(10)	1.391 (19)		1.400 (5)	
C(7)–C(8)	1.344 (22)		1.339 (6)	
C(5)–C(11)	1.490 (15)	1.499 (12)	1.500 (4)	1.501 (1)
C(10)–C(17)	1.507 (17)		1.502 (4)	
C(11)–C(12)	1.416 (18)		1.375 (5)	
C(11)–C(16)	1.370 (21)		1.378 (5)	
C(12)–C(13)	1.364 (20)		1.386 (5)	
C(13)–C(14)	1.355 (24)		1.369 (6)	
C(14)–C(15)	1.320 (22)		1.363 (6)	
C(15)–C(16)	1.385 (18)	1.367 (26)	1.390 (5)	1.377 (9)
C(17)–C(18)	1.359 (24)		1.389 (6)	
C(17)–C(22)	1.363 (19)		1.378 (5)	
C(18)–C(19)	1.391 (20)		1.381 (6)	
C(19)–C(20)	1.374 (22)		1.362 (6)	
C(20)–C(21)	1.339 (26)		1.373 (7)	
C(21)–C(22)	1.373 (20)		1.377 (6)	
C(23)–O(1)	1.158 (20)		1.144 (5)	
C(24)–O(2)	1.156 (19)	1.162 (9)	1.147 (4)	1.146 (2)
C(25)–O(3)	1.172 (23)		1.147 (5)	
M–M	3.126 (1)		3.101 (1)	
M–N(1)′[c]	3.230 (3)		3.208 (3)	
Ct[d]–N(1)	2.263 (12)		2.253 (3)	
Ct–N(2)	1.814 (16)		1.836 (4)	
Ct–C(1)	3.212 (14)	3.214 (3)	3.183 (4)	3.189 (8)
Ct–C(4)	3.216 (14)		3.191 (4)	
Ct–C(6)	2.892 (12)	2.903 (15)	2.922 (3)	2.924 (4)
Ct–C(9)	2.914 (12)		2.927 (3)	
Ct–C(5)	3.444 (12)	3.445 (1)	3.441 (4)	3.442 (1)
Ct–C(10)	3.446 (12)		3.443 (4)	
N(1)–N(2)	2.898 (15)	2.900 (4)	2.909 (4)	2.907 (4)
N(1)–N(2)′[c]	2.903 (14)		2.904 (3)	

[a] Some nonbonding distances of interest are also given. [b] For averaged values, the figures in parentheses are the rms standard deviations. [c] Primed atoms related to umprimed by the symmetry operation $x' = -x, y' = -y, z' = -z$. [d] Ct = center of porphyrin ring.

distance is slightly smaller than the analogous bond length in pyrrole ring 1. In this case, however, the significance of these differences may only be classified as marginal. In normal metalloporphyrin complexes, the Cα-Cβ distance has been found to be remarkably constant at approximately 1.44 Å.[53] The Cβ-Cα-Cm and N-Cα-Cm angles are considerably different in the two rings, but this is probably a factor of the distortion of the macrocycle.

As is normal for metallotetraphenylporphine complexes,[4] the phenyl rings are rotated considerably out of the plane of the macrocycle. The angles between the planes of the phenyl rings and the plane of the macrocycle are listed in Table X. The average carbon-carbon bond distance in the two phenyl rings is 1.37 (3) and 1.377 (9) Å for the rhenium and technetium complexes, respectively.

One O-O intermolecular contact is unusually short. This is the contact O(1)-O(3)″ ($x'' = x, y'' = 0.5 - y, z'' = -0.5 + z$) which is 2.91 Å long. This distance is greater

Table IX. Bond Angles (deg) in $TPP[Re(CO)_3]_2$ and $TPP[Tc(CO)_3]_2$[a]

Angle	$TPP[Re(CO)_3]_2$		$TPP[Tc(CO)_3]_2$	
N(1)–M–N(2)	79.0 (4)		79.2 (1)	
N(1)–M–N(2)'[b]	78.6 (4)		78.6 (1)	
N(1)–M–C(23)	175.7 (7)		176.5 (2)	
N(1)–M–C(24)	95.4 (5)		95.4 (1)	
N(1)–M–C(25)	94.8 (6)		94.8 (1)	
N(2)–M–N(2)'[b]	98.5 (4)		99.6 (1)	
N(2)–M–C(23)	98.3 (5)		99.2 (2)	
N(2)–M–C(24)	171.1 (5)		171.0 (1)	
N(2)–M–C(25)	84.5 (5)		84.6 (1)	
N(2)'[b]–M–C(23)	98.6 (6)		98.7 (1)	
N(2)'[b]–M–C(24)	87.0 (5)		86.3 (1)	
N(2)'[b]–M–C(25)	172.0 (7)		171.3 (2)	
C(23)–M–C(24)	87.6 (7)		86.6 (2)	
C(23)–M–C(25)	88.3 (8)		88.0 (2)	
C(24)–M–C(25)	89.2 (6)		88.6 (2)	
M–N(1)–C(1)	125.9 (7)		125.3 (2)	
M–N(1)–C(4)	124.9 (8)		125.0 (2)	
C(1)–N(1)–C(4)	106.6 (10)		107.2 (2)	
M–N(2)–C(6)	110.0 (9)		110.5 (2)	
M–N(2)–C(9)	129.1 (7)		129.6 (2)	
C(6)–N(2)–C(9)	104.5 (9)		104.3 (2)	
M–N(2)'[b]–C(6)'[b]	125.7 (8)		125.1 (2)	
M–N(2)'[b]–C(9)'[b]	107.2 (8)		107.9 (2)	
N(1)–C(1)–C(2)	107.9 (9)	108.7 (11)	109.4 (2)	109.3 (2)
N(1)–C(4)–C(3)	109.5 (10)		109.1 (2)	
N(1)–C(1)–C(10)'[b]	121.5 (12)	121.9 (5)	123.1 (3)	123.0 (1)
N(1)–C(4)–C(5)	122.2 (12)		123.0 (3)	
C(2)–C(1)–C(10)'[b]	130.5 (11)	129.1 (20)	127.2 (3)	127.4 (2)
C(3)–C(4)–C(5)	127.7 (10)		127.5 (3)	
C(1)–C(2)–C(3)	108.9 (11)	107.9 (15)	106.7 (3)	107.0 (4)
C(2)–C(3)–C(4)	106.8 (11)		107.3 (3)	
N(2)–C(6)–C(7)	109.8 (13)	109.1 (10)	109.4 (3)	109.3 (1)
N(2)–C(9)–C(8)	108.4 (11)		109.3 (3)	
N(2)–C(6)–C(5)	129.9 (10)	129.8 (2)	129.3 (2)	129.0 (4)
N(2)–C(9)–C(10)	129.7 (9)		128.7 (2)	
C(5)–C(6)–C(7)	120.3 (12)	121.1 (11)	121.4 (3)	121.7 (4)
C(8)–C(9)–C(10)	121.9 (12)		121.9 (3)	
C(6)–C(7)–C(8)	107.8 (11)	108.7 (12)	108.6 (3)	108.5 (2)
C(7)–C(8)–C(9)	109.6 (12)		108.3 (3)	
C(4)–C(5)–C(6)	124.6 (11)	124.8 (3)	124.8 (3)	124.7 (1)
C(9)–C(10)–C(1)'[b]	125.0 (11)		124.6 (3)	
C(4)–C(5)–C(11)	118.4 (12)	117.6 (16)	117.8 (3)	117.6 (8)
C(6)–C(5)–C(11)	116.9 (10)		117.2 (3)	
C(1)'[b]–C(10)–C(17)	115.7 (12)		116.8 (3)	
C(9)–C(10)–C(17)	119.3 (9)		118.6 (2)	
C(5)–C(11)–C(12)	120.7 (12)	121.2 (10)	120.8 (3)	120.7 (13)
C(5)–C(11)–C(16)	122.2 (11)		120.5 (3)	
C(10)–C(17)–C(18)	120.0 (11)		120.4 (3)	
C(10)–C(17)–C(22)	121.8 (14)		119.2 (3)	
C(12)–C(11)–C(16)	117.1 (11)	120.0 (13)	118.7 (3)	120.0 (9)
C(11)–C(12)–C(13)	119.8 (14)		121.1 (4)	
C(12)–C(13)–C(14)	120.3 (14)		119.3 (4)	
C(13)–C(14)–C(15)	121.6 (12)		120.5 (4)	
C(14)–C(15)–C(16)	119.7 (15)		120.0 (4)	
C(15)–C(16)–C(11)	121.3 (13)		120.4 (3)	
C(18)–C(17)–C(22)	118.2 (13)		118.4 (3)	
C(17)–C(18)–C(19)	120.8 (13)		120.0 (3)	
C(18)–C(19)–C(20)	119.1 (16)		120.7 (4)	
C(19)–C(20)–C(21)	120.3 (14)		119.9 (4)	
C(20)–C(21)–C(22)	119.8 (14)		119.8 (4)	
C(21)–C(22)–C(17)	121.7 (16)		121.2 (4)	
M–C(23)–O(1)	176.3 (16)	177.8 (13)	176.6 (4)	177.7 (13)
M–C(24)–O(2)	178.6 (13)		177.3 (3)	
M–C(25)–O(3)	178.5 (13)		179.3 (4)	

[a] For averaged values, the figures in parentheses are the rms standard deviations. [b] Primed atoms related to unprimed by the symmetry operation $x' = -x, y' = -y, z' = -z$.

than the sum of the van der Waals radii. This contact does not appear to have any effect on the molecular structure. All other contacts are greater than 3.35 Å with most being greater than 3.5 Å.

Discussion

Although high oxidation state rhenium complexes of porphyrin[33] and phthalocyanine[54] have been prepared, the low oxidation state, out-of-plane, rhenium and technetium complexes of porphyrin are synthesized differently by using the metal carbonyl method.[25] The new metalloporphyrin complexes are unusual in coordination and stereochemistry. Both the homo- and heterodinuclear metalloporphyrin complexes of Re(I) and Tc(I) are prepared for the first time. In these dimetallic complexes the porphyrin acts as a hexadentate ligand, while, in the analogous monometallic com-

Table X. A. Deviation (Å) from Least-Squares Planes for $TPP[Re(CO)_3]_2$ and $TPP[Tc(CO)_3]_2$

	Plane 1 (4 pyrrole N)		Plane 2 (pyrrole 1)		Plane 3 (pyrrole 2)	
	Re	Tc	Re	Tc	Re	Tc
M	−1.429	−1.419	0.666	0.647	1.326	1.314
N(1)	0.0	0.0	0.024	0.022	0.133	0.139
N(2)	0.0	0.0	−0.896	−0.904	−0.011	−0.007
C(1)	0.379	0.360	−0.024	−0.013	−0.240	−0.216
C(2)	0.891	0.917	0.016	−0.001	−0.538	−0.552
C(3)	0.909	0.904	−0.001	0.013	−0.438	−0.418
C(4)	0.369	0.373	−0.015	−0.022	−0.036	−0.030
C(5)	0.345	0.357	−0.206	−0.219	0.028	0.031
C(6)	0.204	0.221	−0.639	−0.652	0.009	0.006
C(7)	0.275	0.288	−0.885	−0.900	−0.004	−0.003
C(8)	0.093	0.103	−1.261	−1.275	−0.003	−0.002
C(9)	−0.094	−0.089	−1.268	−1.278	0.004	0.006
C(10)	−0.289	−0.294	−1.636	−1.645	−0.006	−0.008
N(1)'[a]	0.0	0.0	−1.817	−1.828	–	–
N(2)'[a]	0.0	0.0	–	–	−0.330	−0.339

B. Interplanar Angles (in deg)

	1		2		3		4	
Plane	Re	Tc	Re	Tc	Re	Tc	Re	Tc
2	24.0	24.2	–	–				
3	9.2	9.5	17.0	17.0	–	–		
4	82.5	82.8	63.7	63.9	79.5	79.6	–	–
5	54.6	54.3	72.6	72.6	63.7	63.6	88.5	88.2

Plane 1:[b] 4 Pyrrole nitrogen atoms
Re: $7.198x - 13.017y - 2.972z = 0.0$
Tc: $7.223x - 12.966y - 2.954z = 0.0$
Plane 2: Pyrrole Ring 1 (N(1), C(1)–C(4))
Re: $-9.696x + 8.726y + 6.606z = 0.8962$
Tc: $-9.751x + 8.650y + 6.628z = 0.9032$
Plane 3: Pyrrole Ring 2 (N(2), C(6)–C(9))
Re: $-7.645x + 12.347y + 4.727z = 0.1702$
Tc: $-7.689x + 12.272y + 4.768z = 0.1731$
Plane 4: Phenyl Ring (C(11)–C(16))
Re: $10.317x + 8.127y - 4.536z = -0.5543$
Tc: $10.328x + 8;165y - 4.527z = -0.5606$
Plane 5: Phenyl Ring 2 (C(17)–C(22))
Re: $3.065x - 8.340y + 7.115z = -0.1750$
Tc: $3.084x - 8.368y + 7.091z = -0.1857$

[a] Primed atoms related to unprimed by center of symmetry. [b] Note: All planes are unweighted. x,y,z are in monoclinic fractional coordinates.

plexes, the porphyrin acts as a tridentate ligand. These are rather unusual coordination numbers for the porphyrin ligand.[3] A similar unusual coordination number has also been observed in low oxidation state, out-of-plane rhodium porphyrin complexes.[42] In these rhodium complexes the porphyrin acts either as a bidentate or a tetradentate ligand.

Octahedral[44] coordination was observed in the unusual metalloporphyrin complexes of Re(I) and Tc(I); each metal ion is bonded to three carbonyls and three adjacent pyrrole nitrogen atoms of the porphyrin ring. However, square planar[42] coordination was found in the unusual metalloporphyrin complexes of Rh(I), each metal ion being bonded to two carbonyls and two pyrrole nitrogen atoms. The low oxidation states of these metal ions are presumably stabilized by the carbonyl ligands, and their electronic configurations are consistent (except for the Rh(I) complexes) with the 18-electron rule.[55] Among these out-of-plane unusual metalloporphyrin complexes, only the Re(I) complexes are stable compounds; both the Rh(I) and Tc(I) complexes are thermally unstable. A novel thermal disproportionation reaction (Figure 6) of $(H\text{-}MP)Tc(CO)_3$ and the thermal instability of $MP[Tc(CO)_3]_2$ have been described earlier. The out-of-plane, dimetallic porphyrin complex of Rh(I) is also unstable with respect to the in-plane, square planar Rh(III) porphyrin complex.[41] The mechanisms of these unusual reactions are unknown. However, dissociation and recombination of the metal-carbonyl moieties with the porphyrin ligand could explain the thermal disproportionation of $(H\text{-}MP)Tc(CO)_3$ to $Mp[Tc(CO)_3]_2$ and $H_2MPIXDME$.

The out-of-plane, monorhenium complex of porphyrin can be used as a model for the proposed "sitting-atop" intermediate in metalloporphyrin formation.[56,57] Although homo- and heterodinuclear, out-of-plane, metalloporphyrin complexes of Re and Tc were prepared through the monorhenium complex by further reaction with $Re_2(CO)_{10}$ and $Tc_2(CO)_{10}$, the incorporation of additional mono- and divalent heavy metal ions (Ag^+, Hg^{2+}, and Pb^{2+}) to the monorhenium porphyrin complex did not produce stable complexes.[48] It is of interest that an unusual, stable, out-of-plane, metalloporphyrin complex of mercury(II) was prepared simply by the reaction of mercuric acetate with porphyrin in tetrahydrofuran and methylene chloride. This new metalloporphyrin complex was proposed to have an unusual "double-sandwich" structure.[58] Still another mercury porphyrin, this one containing two mercury(II) atoms per porphyrin, has been prepared.[59] It seems to resemble the bimetallic complexes of rhenium(I) and technetium(I). Further comparisons may prove useful.

The intramolecular rearrangement[46] of the metal-carbonyl moiety among the pyrrole nitrogen atoms in the porphyrin ring is the first fluxional behavior reported for the out-of-plane metalloporphyrins such as these. However, both the inter- and intramolecular ligand site exchanging[60] reactions were responsible for the variable-temperature ^1H NMR spectral changes in the ruthenium monocarbonyl porphyrin complex coordinated with other nitrogen bases. Rotation of phenyl rings[61,62] in the substituted tetraphenylporphine complexes of Ru(II) and In(III) was also observed by variable-temperature ^1H NMR studies. These three different types of fluxional behaviors are very unusual for metalloporphyrins.

One of the major reasons for single-crystal X-ray diffraction analyses of $TPP[Re(CO)_3]_2$ and $TPP[Tc(CO)_3]_2$ was to investigate the possible existence of a metal-metal bonding through the porphyrin "hole" to form a "skewered compound". However, it would appear that for the following reasons the metal-metal interactions, if present, are weak. Firstly, the M-M distance (~3.1 Å) is rather large for a metal-metal bond. Most Re-Re single bond distances are approximately 2.7 Å long,[63] although a value of 3.02 Å has been reported for $Re_2(CO)_{10}$.[64] Secondly, the macrocycle is highly distorted in a way which would maximize the M-M distance. Thirdly, the 18-electron rule[55] is fulfilled without postulating a metal-metal bond.

Experimental Section

Materials. Hemin was purchased from Sigma Chemical Co.; dirhenium decacarbonyl, $Re_2(CO)_{10}$, and ditechnetium decacarbonyl, $Tc_2(CO)_{10}$, were purchased from Pressure Chemical Co.; $Tc_2(CO)_{10}$ is a radioactive material with radioactivity of 5 μCi/mg ($^{43}Tc^{99}$: β^-, 0.292 MeV; half-life, 2.12×10^5 years). Talcum powder was purchased from Fisher Scientific Co., and Sephadex LH-20 was obtained from Pharmacia Fine Chemicals. Decahydronaphthalene (decalin) was purchased from J. T. Baker Chemical Co., treated with concentrated sulfuric acid, neutralized with sodium bicarbonate solution, washed with distilled water, dried over anhydrous calcium chloride overnight, filtered, and further dried over sodium wire; finally it was distilled under vacuum and stored in a Schlenk tube under argon before use. 1,1,2,2-Tetrachloroethane was purchased from Eastman Kodak Co., dried over phosphorus pentoxide, and distilled under vacuum before use. Other organic solvents were commercial reagent grade and were used without further purification.

Physical Measurements. Elemental analyses and molecular weight determinations were performed by Schwarzkopf Microanalytical Laboratory, Woodside, N.Y. 11377. Visible spectra were

measured with a Cary 14 spectrophotometer. Infrared spectra were measured with a Beckman IR-8 spectrophotometer. Mass spectra were obtained on a CEC 21-104 mass spectrometer. Proton magnetic resonance spectra were obtained using Varian T-60 and HA-100 spectrometers; the latter was equipped with a variable-temperature probe and operated at power levels well below saturation. Temperatures were measured with a thermocouple mounted in the probe which was calibrated with ethylene glycol after each set of spectra.

Preparations. Mesoporphyrin IX dimethyl ester,[65] H_2MPIXDME, and *meso*-tetraphenylporphine,[66,67] H_2TPP, were prepared by literature procedures. (Monohydrogen mesoporphyrin IX dimethyl esterato)tricarbonylrhenium(I), (H-MP)$Re(CO)_3$ (I), μ-[mesoporphyrin IX dimethyl esterato]-bis[tricarbonylrhenium(I)], MP$[Re(CO)_3]_2$ (III), μ-[*meso*-tetraphenylporphinato]-bis[tricarbonylrhenium(I)], TPP$[Re(CO)_3]_2$ (IV), and μ-[mesoporphyrin IX dimethyl esterato]-[tricarbonylrhenium(I)][tricarbonyltechnetium(I)], $(OC)_3$ReMPTc$(CO)_3$ (V) were prepared as previously reported.[43-45]

[Monohydrogen mesoporphyrin IX dimethyl esterato]tricarbonyltechnetium(I), (H-MP)Tc$(CO)_3$ (VI). A 45.5-mg sample of H_2MPIXDME (7.58×10^{-2} mmol) and 21.25 mg (4.46×10^{-2} mmol) of $Tc_2(CO)_{10}$ were mixed in 10 ml of decalin and heated under argon in a 150° oil-bath for approximately 2 hr. Completion of the reaction was determined by visible spectroscopy. When absorption at 388 nm (Soret band) and 473 nm reached maxima, the reaction was stopped. The decalin solution was cooled, centrifuged, and decanted, and the supernatant evaporated to dryness under vacuum by using a Molecular Still apparatus. The resulting solid was then dissolved in benzene and chromatographed on a talcum column. Three bands were eluted from the column by benzene–cyclohexane (50/50), dichloromethane, and acetone, respectively. A small amount of chocolate colored material was followed by a large pale green band and finally by a small amount of red compound. Visible spectroscopy showed the first and third bands to be MP$[Tc(CO)_3]_2$ (VII) and H_2MPIXDME. A dichloromethane solution of the second band was evaporated to small volume under a stream of nitrogen, centrifuged, and decanted. The supernatant was evaporated to dryness and washed with *n*-pentane to give an air stable, dark greenish brown solid of VI (24.15 mg, 41.0% yield), mp 181–182°. Anal. Calcd for $TcC_{39}H_{41}N_4O_7$: N, 7.22; Tc, 12.75; mol wt, 776.8. Found: N, 7.34; Tc, 12.37; mol wt, 767 (measured by vapor pressure osmometry in chloroform).

μ-[Mesoporphyrin IX dimethyl esterato]-bis[tricarbonyltechnetium(I)], MP$[Tc(CO)_3]_2$ (VII). The preparation of this compound was similar to that of VI, except the ratio of reactants was changed. H_2MPIXDME (20.6 mg, 3.49×10^{-2} mmol) and $Tc_2(CO)_{10}$ (19.5 mg, 4.08×10^{-2} mmol) were mixed in 10 ml of decalin and heated under argon in a 150° oil-bath for approximately 5 hr. Completion of the reaction was determined by visible spectroscopy; stepwise absorption changes of the reaction mixture were observed as shown in Figure 3. When the absorptions at 396 nm (Soret band) and 507 nm reached maxima, the reaction was stopped. The decalin solution was centrifuged, decanted, and evaporated in vacuo; the resulting solid was dissolved in benzene and chromatographed on a talcum column. A large chocolate colored band was eluted with a benzene–cyclohexane (50/50) solution. This solution was evaporated to dryness, dissolved in dichloromethane, centrifuged, and decanted. Finally it was evaporated to dryness and washed with *n*-pentane to give a dark reddish brown solid of VII (21.20 mg, 65.8% yield), mp 227–229°. Anal. Calcd for $Tc_2C_{42}H_{40}N_4O_{10}$: C, 52.60; H, 4.18; N, 5.84; Tc, 20.65; mol wt, 958.0. Found: C, 52.44; H, 4.08; N, 5.92; Tc, 20.54; mol wt, ~1062 (measured by vapor pressure osmometry in acetone).

μ-[*meso*-Tetraphenylporphinato]-bis[tricarbonyltechnetium(I)], TPP$[Tc(CO)_3]_2$ (VIII). The preparation of this compound was similar to that of VII, except the porphyrin ligand was changed. H_2TPP (23.0 mg, 3.75×10^{-2} mmol) and $Tc_2(CO)_{10}$ (20.6 mg, 4.31×10^{-2} mmol) were mixed in 10 ml of decalin and refluxed under argon for approximately 2 hr. Completion of the reaction was determined by visible spectroscopy. The visible spectrum of this mixture after 2 hr refluxing was rather similar to that of VII. The crude product was isolated from the decalin solution in a similar manner as that of VII and chromatographed on a Sephadex LH-20 column. A reddish brown colored band was eluted with a benzene–cyclohexane (50/50) solution. This solution was concentrated to small volume, centrifuged, and decanted. Finally it was evaporated to dryness, washed with *n*-pentane, and crystallized from dichloromethane–chloroform solution to give reddish brown crystals of VIII (23.81 mg, 65.1% yield), mp 323–325°. These crystals were used for X-ray diffraction analyses.

[Monohydrogen *meso*-tetraphenylporphinato]tricarbonylrhenium(I), (H-TPP)Re$(CO)_3$ (II). A 207.5-mg sample of H_2TPP (0.338 mmol) and 100 mg (0.157 mmol) $Re_2(CO)_{10}$ in 20 ml of decalin were refluxed under argon for approximately 3 hr. Completion of the reaction was determined by visible spectroscopy. The crude product was isolated from the decalin solution in a similar manner as that of VII, and chromatographed on a Sephadex LH-20 column. A yellowish brown colored band was eluted with cyclohexane. This solution was concentrated to small volume, centrifuged, and decanted. The supernatant was evaporated to dryness, washed with *n*-pentane, and crystallized from absolute alcohol–chloroform solution to give an air stable, dark greenish brown solid of II (140.3 mg, 50.6% yield), mp 302–304°. Anal. Calcd for $ReC_{47}H_{29}N_4O_3$: C, 63.80; H, 3.29; N, 6.34; Re, 21.08; mol wt, 883.2. Found: C, 63.78; H, 3.57; N, 6.47; Re, 21.43; mol wt, 840 (in dibromomethane).

X-Ray Study. Crystals of μ-[*meso*-tetraphenylporphinato]-bis[tricarbonylrhenium(I)] TPP$[Re(CO)_3]_2$ (IV), $C_{50}H_{28}O_6N_4Re_2$, were grown from a dioxane solution. The crystals grew as elongated plates with the most prominent faces being {100}, and bounded by {010} and {011}. The crystal used for intensity measurements had dimensions 0.03 and 0.08 mm in the direction of *a* and *b*, respectively, while the long dimension (approximately parallel to *c*) was 0.28 mm. The crystals appear green in reflected light.

Crystals of μ-[*meso*-tetraphenylporphinato]-bis[tricarbonyltechnetium(I)], TPP$[Tc(CO)_3]_2$ (VIII), $C_{50}H_{28}O_6N_4Tc_2$, exhibited two different crystal habits. One form was the same as that ited two different crystal habits. One form was the same as that found for the rhenium compound while the other form was much more complex. These crystals were again plates with the prominent faces being of the form {100}, and bounded by {011} and the faces [111], [$\bar{1}\bar{1}$1], [1$\bar{1}$1], and [$\bar{1}\bar{1}\bar{1}$]. Two corners were truncated by faces of the form {010}. Crystals of this form were grown from chloroform and dichloromethane. The crystal chosen for intensity measurements was of this form and had dimensions of $0.18 \times 0.37 \times 0.32$ mm. Both forms appeared green in reflected light and gave identical space group and cell dimensions. Crystals of both complexes were mounted in glass capillaries.

Crystal data for both the rhenium and technetium complexes are listed in Table IV. Also listed are some of the experimental conditions used in the intensity measurements. Cell dimensions were determined by least squares, minimizing the differences between observed and calculated 2θ values. For both complexes Mo Kα radiation, monochromatized by pyrolytic graphite, was used. The 2θ values were measured on a Syntex-Datex automated four-circle diffractometer. In the case of TPP$[Tc(CO)_3]_2$, the 2θ values for 19 Mo Kα_1 reflections (λ 0.70926 Å) were measured. For six of these, the Kα_1–Kα_2 doublet was sufficiently resolved to measure the 2θ values for the Kα_2 reflextions (λ 0.71254 Å). In the case of TPP$[Re(CO)_3]_2$, the doublet was not well resolved and 40 2θ values were measured assuming the wavelength to be Mo K$\bar{\alpha}$ (λ 0.71069 Å). The densities were determined by the flotation method in an aqueous thallous formate solution. The two complexes are isomorphous. In both cases the choice of space group $P2_1/c$ was uniquely determined by the systematic absences.

Intensity data were collected on the Datex-Syntex diffractometer. The data in each case were collected by the θ–2θ scan method, monitoring the intensity scale by remeasuring a group of five standard reflections periodically. For both complexes there were no significant or systematic trends in the intensities of these check reflections and no corrections were made. Backgrounds at either end of the scan range were collected for half the scan time. Only reflections with $I \geq 3\sigma_I$ were used in the analyses. The standard deviation σ_I was determined in terms of the statistical variances of the counts as $\sigma_1^2 = \sigma_1^2(\text{count}) + K^2(S + B1 + B2)^2$, where *S*, *B*1, and *B*2 are the observed counts for the scan and two backgrounds, respectively. σ_I^2(count) is the variance determined purely from counting statistics. The values of *K*, the so-called stability constant, were determined empirically. The intensities were corrected for coincidence using the method of Sletten, Sletten, and Jensen.[68] Absorption effect corrections were applied to both complexes. In

the case of TPP[Tc(CO$_3$]$_2$, where the corrections were small, a numerical integration method was used. In the case of the rhenium complex, the more accurate analytical correction technique of De Meulenaer and Tompa was used.[69] Transmission factors ranged from 0.61 to 0.86 for TPP[Re(CO)$_3$]$_2$ and from 0.85 to 0.93 for TPP[Tc(CO)$_3$]$_2$. Structure factors were calculated in the usual way, assuming an ideally imperfect monochromator.

Determination and Refinement of the Structures. Because there are only two molecules in the unit cell of space group $P2_1/c$, the complex in both cases must be centrosymmetric. However, no atom is constrained to be at a special position. The positions of the metal atoms were found in each case from a Patterson synthesis. The positions of the remaining 30 non-hydrogen atoms in the asymmetric unit were found from a series of ΔF Fourier maps.

Least-squares refinement using block diagonal and finally full-matrix methods[70] was carried out. The function minimized was $\Sigma w(F_o - F_c)^2$, where $w = 1/\sigma_F{}^2$. Initially isotropic temperature factors were used, but in later refinement cycles all non-hydrogen atoms were assumed to have anisotropic thermal motion.

After several cycles of refinement of the non-hydrogen atoms, ΔF syntheses were calculated in an effort to locate hydrogen atoms. In the case of the rhenium complex, the positions of most of the 14 hydrogen atoms could not be located with certainty, so calculated positions for all of them were used and were not refined by least squares. A bond length of 1.0 Å was assumed. In the case of the technetium complex, the hydrogen atoms could be located and these positions were refined, assuming isotropic thermal motion.

In the final cycles of full-matrix least-squares refinement, computer memory limitations necessitated refining the parameters in two blocks. In the first block, all atoms except those belonging to the phenyl groups were refined. In the other block, the metal atom and the atoms of the phenyl group were refined. The final R values are given in Table IV.

Corrections were made for anomalous dispersion for the metal atom in each case.[71] Scattering factors were from the International Tables.[72] The metal ions were assumed to be in the zero ionization state.

The data were examined by the method of Housty and Clastre.[73] No evidence of secondary extinction was found and no correction for this effect was made.

Final difference syntheses were calculated for both compounds. In the case of TPP[Tc(CO)$_3$]$_2$ the maximum residual electron density was 0.5 e/Å^3, while for TPP[Re(CO)$_3$]$_2$ the maximum peak was 1.5 e/Å^3. Both peaks were near the metal ions and were not considered of any physical significance.

The computer programs used have been previously listed.[74,75] The final positional and thermal parameters are listed in Tables V and VI, while the root-mean-square components of thermal displacement along the principal axis of the thermal ellipsoids are given in Table VII. Tables of observed and calculated structure factors are available. See paragraph at end of paper regarding supplementary material.

Acknowledgment. This research project was supported in part by both the National Science Foundation under Grant No. GP-28685 and the Office of Naval Research under Grant No. NR 356-559. The authors wish to thank Dr. Allen E. Gebala for many helpful discussions. Crystallographic investigations were supported by the Robert A. Welch Foundation Grant A-328 and the Texas Agricultural Experiment Station. Crystallographic calculations were facilitated by the CRYSNET system, supported by the National Science Foundation GJ33248X.

Supplementary Material Available. A listing of structure factor amplitudes will appear following these pages in the microfilm edition of this volume of the journal. Photocopies of the supplementary material from this paper only or microfiche (105 × 148 mm, 24× reduction, negatives) containing all of the supplementary material for the papers in this issue may be obtained from the Journals Department, American Chemical Society, 1155 16th St., N.W., Washington D.C. 20036. Remit check or money order for $4.50 for photocopy or $2.50 for microfiche, referring to code number JACS-75-3952.

References and Notes

(1) Unusual Metalloporphyrins XXIII.
(2) (a) Department of Chemistry; (b) Department of Biochemistry and Biophysics, Texas Agricultural Experiment Station.
(3) J. E. Falk, "Porphyrins and Metalloporphyrins", Elsevier, New York, N.Y., 1964.
(4) E. B. Fleischer, *Acc. Chem. Res.*, **3**, 105 (1970).
(5) P. Hambright, *Coord. Chem. Rev.*, **6**, 247 (1971).
(6) L. J. Boucher, *Coord. Chem. Rev.*, **7**, 289 (1972).
(7) D. Ostfeld and M. Tsutsui, *Acc. Chem. Res.*, **7**, 52 (1974).
(8) A. D. Adler, Ed., "The Chemical and Physical Behavior of Porphyrin Compounds and Related Structures", *Ann. N.Y. Acad. Sci.*, **206** (1973).
(9) C. K. Chang and T. G. Traylor, *J. Am. Chem. Soc.*, **95**, 5810, 8475 8477 (1973).
(10) D. V. Stynes, H. C. Stynes, B. R. James, and J. A. Ibers, *J. Am. Chem. Soc.*, **95**, 4087 (1973).
(11) B. B. Wayland, J. V. Minkiewicz, and M. E. Abd-Elmageed, *J. Am. Chem. Soc.*, **96**, 2795 (1974).
(12) J. P. Collman, R. R. Gagne, and C. A. Reed, *J. Am. Chem. Soc.*, **96**, 2629 (1974).
(13) L. P. Vernon and G. R. Seely, Ed., "The Chlorophylls: Physical, Chemical, and Biological Properties", Academic Press, New York and London, 1966.
(14) E. Antonini and M. Brunori, "Hemoglobin and Myoglobin in Their Reactions with Ligands", North-Holland/American Elsevier, 1971.
(15) R. Lemberg and K. Barrett, "Cytochromes", Academic Press, London and New York, 1973.
(16) E. L. Smith, "Vitamin B_{12}", 3rd ed, Wiley, New York, N.Y., 1965.
(17) G. N. Schrauzer, *Acc. Chem. Res.*, **1**, 97 (1968).
(18) A. Goldberg and C. Rimington, "Diseases of Porphyrin Metabolism", Thomas, Springfield, Mass., 1962.
(19) F. Gutmann and L. E. Lyons, "Organic Semiconductors", Wiley, New York, N.Y., 1967.
(20) A. D. Adler, *J. Polym. Sci., Part C*, **29**, 73 (1970).
(21) J. P. Macquet and T. Theophanides, *Can. J. Chem.*, **51**, 219 (1972).
(22) G. A. Kyriazis, H. Balin, and R. L. Lipson, *Am. J. Obstet. Gynecol.*, 376 (1973).
(23) E. B. Fleischer and M. Krishnamurthy, *J. Am. Chem. Soc.*, **94**, 1382 (1972).
(24) C. P. Wong, R. F. Venteicher, and W. D. Horrocks, Jr., *J. Am. Chem. Soc.*, **96**, 7149 (1974).
(25) M. Tsutsui, M. Ichikawa, F. Vohwinkel, and K. Suzuki, *J. Am. Chem. Soc.*, **88**, 854 (1966).
(26) M. Tsutsui, R. A. Velapoldi, K. Suzuki, F. Vohwinkel, M. Ichikawa, and T. Koyano, *J. Am. Chem. Soc.*, **91**, 6262 (1969).
(27) E. B. Fleischer and N. Sadasivan, *Chem. Commun.*, 159 (1967).
(28) B. C. Chow and I. A. Cohen, *Bioinorg. Chem.*, **1**, 57 (1971).
(29) N. Sadasivan and E. B. Fleischer, *J. Inorg. Nucl. Chem.*, **30**, 591 (1968).
(30) J. W. Buchler, G. Eikelmann, L. Puppe, K. Rohbock, H. H. Schnechage, and D. Weck, *Justus Liebigs Ann. Chem.*, **745**, 135 (1971).
(31) A. D. Adler, F. R. Longo, F. Kampas, and J. Kim, *J. Inorg. Nucl. Chem.*, **32**, 2443 (1970).
(32) J. W. Buchler and K. Rohbock, *Inorg. Nucl. Chem. Lett.*, **8**, 1073 (1972).
(33) J. W. Buchler, L. Puppe, K. Rohbock, and H. H. Schneehage, *Chem. Ber.*, **106**, 2710 (1973).
(34) J. W. Buchler and K. Rohbock, *J. Organomet. Chem.*, **65**, 223 (1974).
(35) J. W. Buchler, L. Puppe, K. Rohbock, and H. H. Schneehage, *Ann. N.Y. Acad. Sci.*, **206**, 116 (1973).
(36) E. B. Fleischer and T. S. Srivastava, *Inorg. Chim. Acta*, **5**, 151 (1971).
(37) T. S. Srivastava and E. B. Fleischer, *J. Am. Chem. Soc.*, **92**, 5518 (1970).
(38) J. J. Bonnet, S. S. Eaton, G. R. Eaton, R. H. Holm, and J. A. Ibers, *J. Am. Chem. Soc.*, **95**, 2141 (1973).
(39) E. B. Fleischer and D. Lavalle, *J. Am. Chem. Soc.*, **89**, 7132 (1967).
(40) H. Ogoshi, T. Omura, and Z. Yoshida, *J. Am. Chem. Soc.*, **95**, 1666 (1973).
(41) Z. Yoshida, H. Ogoshi, T. Omura, E. Watanabe, and T. Kurosaki, *Tetrahedron Lett.*, **11**, 1077 (1972).
(42) A. Takenaka, Y. Sasada, T. Omura, H. Ogoshi, and Z. Yoshida, *J. Chem. Soc., Chem. Commun.*, 792 (1973).
(43) D. Ostfeld, M. Tsutsui, C. P. Hrung, and D. C. Conway, *J. Am. Chem. Soc.*, **93**, 2548 (1971).
(44) D. Cullen, E. Meyer, T. S. Srivastava, and M. Tsutsui, *J. Am. Chem. Soc.*, **94**, 7603 (1972).
(45) M. Tsutsui and C. P. Hrung, *J. Am. Chem. Soc.*, **95**, 5777 (1973).
(46) M. Tsutsui and C. P. Hrung, *J. Am. Chem. Soc.*, **96**, 2638 (1974).
(47) L. M. Jackson and S. Sternhell, "Applications of Nuclear Magnetic Resonance Spectroscopy in Organic Chemistry", 2nd ed, Pergamon, New York, N.Y., 1969, p 129.
(48) D. Ostfeld, M. Tsutsui, C. P. Hrung, and D. C. Conway, *J. Coord. Chem.*, **2**, 101 (1972).
(49) F. A. Cotton, *Acc. Chem. Res.*, **1**, 257 (1968).
(50) M. Tsutsui, D. Ostfeld, and L. Hoffman, *J. Am. Chem. Soc.*, **93**, 1820 (1971).
(51) V. W. Day, B. R. Stults, E. L. Tasset, R. O. Day, and R. S. Marianelli, *J. Am. Chem. Soc.*, **96**, 2650 (1974).
(52) P. A. Loach and M. Calvin, *Biochemistry*, **2**, 363 (1963).
(53) J. L. Hoard, *Science*, **174**, 1295 (1971).
(54) H. P. Bonlecka, *Rocz. Chem.*, **41**, 1703 (1967).
(55) P. R. Mitchell and R. V. Parish, *J. Chem. Educ.*, **46**, 811 (1969).
(56) E. B. Fleischer, E. I. Choi, P. Hambright, and A. Stone, *Inorg. Chem.*, **3**, 1284 (1964).
(57) H. Baker, P. Hambright, and L. Wagner, *J. Am. Chem. Soc.*, **95**, 5942 (1973).

(58) M. F. Hudson and K. M. Smith, *J. Chem. Soc., Chem. Commun.*, 515 (1973).
(59) M. F. Hudson and K. M. Smith, *Tetrahedron Lett.*, 2223 (1974).
(60) S. S. Eaton, G. R. Eaton, and R. H. Holm, *J. Organomet. Chem.*, **39**, 179 (1972).
(61) W. Bhatti, M. Bhatti, S. S. Eaton, and G. R. Eaton, *J. Pharm. Sci.*, **62**, 1574 (1973).
(62) S. S. Eaton and G. R. Eaton, *J. Chem. Soc., Chem. Commun.*, 576 (1974).
(63) F. A. Cotton, *Acc. Chem. Res.*, **2**, 240 (1969).
(64) N. I. G. Gapotchenko, N. V. Alekseev, N. E. Kolobova, K. N. Anisimov, I. A. Ronova, and A. A. Johansson, *J. Organomet. Chem.*, **35**, 319 (1972).
(65) A. H. Corwin and J. G. Erdman, *J. Am. Chem. Soc.*, **68**, 2473 (1946).
(66) A. D. Adler, F. R. Longo, J. D. Finarelli, J. Goldmacher, J. Assour, and L. Korsakoff, *J. Org. Chem.*, **32**, 476 (1967).
(67) G. H. Barnett, M. F. Hudson, and K. M. Smith, *Tetrahedron Lett.*, 2887 (1973).
(68) E. Sletten, J. Sletten, and L. H. Jensen, *Acta Crystallogr., Sect. B*, **25**, 1330 (1969).
(69) J. De Meulenaer and H. Tompa, *Acta Crystallogr.*, **19**, 1014 (1965).
(70) W. R. Busing, K. O. Martin, and H. Levy, ORFLS, A Fortran Crystallographic Least-Squares Program, Report ORNL-TM-305, Oak Ridge National Laboratory, Oak Ridge Tenn.
(71) D. T. Cromer and D. Liberman, *J. Chem. Phys.*, **53**, 1891 (1970).
(72) D. T. Cromer, "International Tables for X-Ray Crystallography", Vol. IV, in press.
(73) J. Housty and J. Clastre, *Acta Crystallogr.*, **10**, 695 (1957).
(74) D. L. Cullen and E. F. Meyer, Jr., *J. Am. Chem. Soc.*, **96**, 2095 (1974).
(75) D. L. Cullen and E. F. Meyer, Jr., *Acta Crystallogr., Sect. B*, **29**, 2507 (1973).

Binary Mixed Dioxygen Dinitrogen Complexes of Nickel, Palladium, and Platinum, $(O_2)M(N_2)_n$ (where M = Ni, Pd, or Pt; n = 1 or 2)

G. A. Ozin* and W. E. Klotzbücher

Contribution from the Lash Miller Chemistry Laboratories and Erindale College, University of Toronto, Toronto, Ontario, Canada. *Received November 25, 1974*

Abstract: The products of the cocondensation reactions of Ni, Pd, and Pt atoms with mixtures of O_2, N_2 and Ar at 6–10°K are investigated by matrix isolation infrared spectroscopy and are shown to be binary mixed dioxygen dinitrogen complexes of the form $(O_2)_xM(N_2)_y$. From the number and frequencies of the N–N and O–O stretching modes compared to the parent molecules $M(N_2)_n$ and $M(O_2)_m$ (where M = Ni, n = 1–4; M = Pd, Pt, n = 1–3; M = Ni, Pd, Pt, m = 1 or 2), their ligand concentration and warm-up behavior and $^{14}N_2$–$^{14}N^{15}N$–$^{15}N_2$–$^{16}O_2$–Ar and $^{16}O_2$–$^{16}O^{18}O$–$^{18}O_2$–$^{14}N_2$–Ar isotope multiplet patterns, the reaction products are established to be $(O_2)M(N_2)$ and $(O_2)M(N_2)_2$ containing "side-on" bonded dioxygen and "end-on" bonded dinitrogen in both complexes. Isotopic frequencies are computed for the ligand stretching and metal–ligand stretching modes of the individual complexes using a MVFF approximation and are found to be in close agreement with the observed values. The resulting bond stretching force constants enable one to gain a unique insight into the bonding of N_2 and O_2 to a transition metal in a situation where both ligands are competing for the same bonding electrons.

In a preliminary communication[1] we reported matrix infrared spectroscopic evidence for binary mixed dioxygen dinitrogen complexes of nickel formed in the cocondensation reactions of nickel atoms with $O_2/N_2/Ar$ mixtures. At that time, the mode of attachment of the O_2 and N_2 ligands to the metal had not been established. Moreover, the nature of the bonding of O_2 and N_2 simultaneously to a common metal atom remained an unanswered question. Since our original communication we have extended these experiments to include Pd and Pt and have been able to show that complexes of the form $(O_2)M(N_2)_n$ (where n = 1 or 2) exist for all members of the group. Without exception the complexes appear to contain dioxygen bonded in a side-on fashion and dinitrogen bonded in an end-on fashion to the central metal atom. Having obtained spectroscopic data for the complete group of complexes, we are now in a position to examine trends in their vibrational spectra, force constants, structures, stabilities, and bonding properties. In this paper we report such data.

Experimental Section

Monoatomic Ni and Pd vapors were generated by directly heating a 0.010-in. ribbon filament of the metal with ac in a furnace which has been described previously.[2] Platinum vapor was obtained by heating a 0.060-in. tungsten rod around the center of which were wound several turns of 0.010 in. Pt wire. The nickel, palladium, and platinum metal (99.99%) were supplied by McKay Inc., N.Y. Research grade $^{16}O_2$ (99.99%), $^{14}N_2$ (99.99%), and Ar (99.99%) were supplied by Matheson. Isotopically enriched $^{18}O_2$ (93%) was supplied by Miles Research Laboratories and $^{15}N_2$ (99.5%) by Prochem. Statistically scrambled mixtures of $^{16}O_2$–$^{16}O^{18}O$–$^{18}O_2$ and $^{14}N_2$–$^{14}N^{15}N$–$^{15}N_2$ were prepared by subjecting $^{16}O_2$–$^{18}O_2$ and $^{14}N_2$–$^{15}N_2$ mixtures of about 200 Torr to a continuous tesla discharge. The scrambling process and concentration ratios were monitored by gas phase Raman measurements.

The rate of metal atom deposition was continuously followed and controlled using a quartz crystal microbalance.[3a] The deposition rate was set such that the probability of a metal atom having another metal atom as nearest neighbor in the argon lattice was less than 10^{-3}. Matrix gas flows, controlled by a calibrated micrometer needle valve, were maintained in the range 2–8 mmol/hr. In the infrared experiments the matrices were deposited on a CsI window cooled to either 6°K by an Air Products liquid helium cryotip transfer system or to 12°K by means of an Air Products Displex closed cycle helium refrigerator. Ir spectra were recorded using Perkin-Elmer 621 and 180 spectrophotometers. Normal coordinate calculations were performed using a modified version of Schachtschneider's GMAT and EIGV programs for the MVFF analysis.[3b]

Results

The results for the $M(N_2)_n$ and $M(O_2)_m$ complexes have already been described in detail.[4-6] As some of the data are relevant to the present study, brief references to this earlier work will be necessary for a thorough appreciation of the $(O_2)M(N_2)_n$ problem. Each metal provides its own set of experimental difficulties and subtleties of spectral interpretation, so we will describe each in turn.

Nickel–Nitrogen Reactions. The spectrum obtained on depositing nickel atoms into a $^{14}N_2$:Ar = 1:100–1:200 matrix shows all the lines associated with the known com-